Journal of the Physical Society of Japan
Vol. 68, No. 12, December, 1999, pp. 3994–4008

Effective-Mass Theory of Carbon Nanotubes with Vacancy

Tsuneya ANDO, Takeshi NAKANISHI[1] and Masatsura IGAMI[2]

Institute for Solid State Physics, University of Tokyo
7–22–1 Roppongi, Minato-ku, Tokyo 106-8666

[1] *The Institute of Physical and Chemical Research (RIKEN)*
2–1 Hirosawa, Wako, Saitama 351-0198

[2] *Institute of Materials Science, University of Tsukuba,*
1–1–1 Tennodai, Tsukuba, Ibaraki 305-8573

(Received July 7, 1999)

Effects of impurities with a strong and short-range potential are studied in carbon nanotubes within a $\boldsymbol{k}\cdot\boldsymbol{p}$ scheme. The calculated conductance approaches those obtained for nanotubes with a lattice vacancy when the strength of the potential is sufficiently large. The conductance at $\epsilon=0$ is analytically shown to be quantized into zero, one, and two times of the conductance quantum $e^2/\pi\hbar$ depending on the difference in the number of vacancies at A and B sublattices in nanotubes with a sufficiently large diameter.

KEYWORDS: graphite, carbon nanotube, vacancy, conductance, effective-mass theory

§1. Introduction

A carbon nanotube (CN) is composed of concentric tubes of rolled two-dimensional (2D) graphite sheets, on which hexagons are arranged in a helical fashion about the axis.[1)] The diameter of each tube ranges from 20 to 300 Å and the maximum length exceeds 1μm. Single-wall nanotubes having a diameter lying between 7 and 16 Å can be synthesized also.[2,3)] The purpose of this paper is to study effects of a strong and short-range perturbation including lattice vacancies in a $\boldsymbol{k}\cdot\boldsymbol{p}$ scheme.

Various calculations have been performed to predict energy bands.[4−12)] It has been found that their characteristic properties are reproduced in a $\boldsymbol{k}\cdot\boldsymbol{p}$ method.[13)] The $\boldsymbol{k}\cdot\boldsymbol{p}$ scheme is quite powerful in the study of effects of external fields such as magnetic and electric fields. In fact, it has been successful in the study of magnetic properties including the Aharonov-Bohm effect on the band gap,[14)] optical absorption spectra,[15,16)] and lattice instabilities in the presence and absence of a magnetic field.[17,18)]

Transport properties of CN's are interesting because of their unique topological structure. There have been some reports on experimental study of transport in C-N bundles.[19)] Quite recently, measurements of magnetotransport of a single nanotube became possible.[20,21)] The tunneling at a finite-length CN[22)] and a connection of different CN's[23−26)] were calculated. The conductivity was calculated in a constant-relaxation-time approximation.[27)] A calculation of the conductance of armchair nanotubes with a single vacancy was reported also.[28)]

The conductivity of CN's was previously calculated using a Boltzmann transport equation[29)] and in Landauer' approach[30)] for a model of short-range scatterers. The results were shown to have a close connection with transport in a 2D graphite sheet.[31)] In a previous paper,[32)] effects of impurity scattering in CN's were studied in detail and the absence of backward scattering was predicted and proved rigorously except for scatterers having a potential range smaller than the lattice constant. This intriguing fact was related to Berry's phase acquired by a rotation in the wave vector space in the system described by a $\boldsymbol{k}\cdot\boldsymbol{p}$ Hamiltonian which is same as Weyl's equation for a neutrino.[33)] The conductance was calculated in a tight-binding model and the result confirmed the absence of backward scattering when the potential is sufficiently small, i.e., the maximum value is smaller than the typical width of the conduction and valence bands.[34,35)] A quantized conductance was observed in a multi-wall nanotube.[36)]

Quite recently, effects of scattering by a vacancy were studied in metallic armchair nanotubes in the presence and absence of a magnetic field.[37−40)] The conductance was shown to be quantized into zero, one, and two times of the conductance quantum $e^2/\pi\hbar$ depending on the type of the vacancy. In this paper we shall extend a $\boldsymbol{k}\cdot\boldsymbol{p}$ scheme so as to discuss effects of strong and localized potentials including those of lattice vacancies and present analytic derivation of the intriguing conductance quantization in the presence of vacancies.

§2. Effective-Mass Approximation

2.1 Hamiltonian

The structure of a 2D graphite is shown in Fig. 1 together with the first Brillouin zone and the coordinates system to be used in the following. A unit cell contains two carbon atoms denoted as A and B. In a 2D graphite, two bands having approximately a linear dispersion cross the Fermi level (chosen at $\varepsilon=0$) at K and K' points of the first Brillouin Zone. The wave vectors of the K and K' points are given by $\boldsymbol{K}=(2\pi/a)(1/3,1/\sqrt{3})$ and $\boldsymbol{K}'=(2\pi/a)(2/3,0)$.

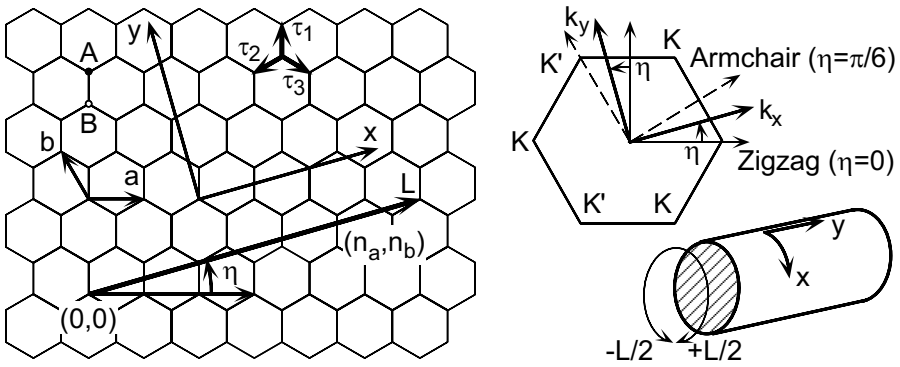

Fig. 1 (a) Lattice structure of two-dimensional graphite sheet. η is the chiral angle. The coordinates are chosen in such a way that x is along the circumference of a nanotube and y is along the axis. (b) The first Brillouin zone and K and K' points. (c) The coordinates for a nanotube.

In the vicinity of the Fermi level, electronic states are described by the Schrödinger equation given by

$$\mathcal{H}\boldsymbol{F}(\boldsymbol{r}) = \varepsilon \boldsymbol{F}(\boldsymbol{r}), \tag{2.1}$$

with

$$\mathcal{H} = \mathcal{H}_0 + V, \tag{2.2}$$

where

$$\mathcal{H}_0 = \begin{array}{c} \begin{matrix} KA & KB & K'A & K'B \end{matrix} \\ \begin{pmatrix} 0 & \gamma(\hat{k}_x - \mathrm{i}\hat{k}_y) & 0 & 0 \\ \gamma(\hat{k}_x + \mathrm{i}\hat{k}_y) & 0 & 0 & 0 \\ 0 & 0 & 0 & \gamma(\hat{k}_x + \mathrm{i}\hat{k}_y) \\ 0 & 0 & \gamma(\hat{k}_x - \mathrm{i}\hat{k}_y) & 0 \end{pmatrix} \end{array}, \tag{2.3}$$

and

$$\boldsymbol{F}(\boldsymbol{r}) = \begin{pmatrix} \boldsymbol{F}^K(\boldsymbol{r}) \\ \boldsymbol{F}^{K'}(\boldsymbol{r}) \end{pmatrix}, \tag{2.4}$$

with

$$\boldsymbol{F}^K(\boldsymbol{r}) = \begin{pmatrix} F^{KA}(\boldsymbol{r}) \\ F^{KB}(\boldsymbol{r}) \end{pmatrix}, \quad \boldsymbol{F}^{K'}(\boldsymbol{r}) = \begin{pmatrix} F^{K'A}(\boldsymbol{r}) \\ F^{K'B}(\boldsymbol{r}) \end{pmatrix}. \tag{2.5}$$

Here, F^{KA} and F^{KB} describe the amplitude at an A and B site, respectively, for the component at the K point, and $F^{K'A}$ and $F^{K'B}$ describe that for the K' point.

For the discussion of scattering from short-range scatterers localized at several lattice points, it is more convenient to choose the representation in which the $(4,4)$ matrix Hamiltonian is rewritten as

$$\mathcal{H}_0 = \begin{array}{c} \begin{matrix} KA & K'A & KB & K'B \end{matrix} \\ \begin{pmatrix} 0 & 0 & \gamma(\hat{k}_x - \mathrm{i}\hat{k}_y) & 0 \\ 0 & 0 & 0 & \gamma(\hat{k}_x + \mathrm{i}\hat{k}_y) \\ \gamma(\hat{k}_x + \mathrm{i}\hat{k}_y) & 0 & 0 & 0 \\ 0 & \gamma(\hat{k}_x - \mathrm{i}\hat{k}_y) & 0 & 0 \end{pmatrix} \end{array}. \tag{2.6}$$

An eigenstate of the Hamiltonian is written as

$$\boldsymbol{F}_{snk}(\boldsymbol{r}) = \frac{1}{\sqrt{AL}} \boldsymbol{f}_{snk} \exp[\mathrm{i}\kappa(n)x + \mathrm{i}ky], \tag{2.7}$$

where A is the length of the nanotube, $s=+1$ denotes a conduction band, $s=-1$ a valence band, k is the wave vector in the direction of the axis, and $\kappa(n)$ is that in the circumference direction, i.e.,

$$\kappa(n) = \frac{2\pi n}{L}, \tag{2.8}$$

with an integer n and the circumference L. The four-component eigenvector $\boldsymbol{f}_{snk}$ is normalized as $|\boldsymbol{f}_{snk}| = 1$ and satisfies

$$\mathcal{H}_0(nk)\boldsymbol{f}_{snk} = \varepsilon_{snk}\boldsymbol{f}_{snk}, \tag{2.9}$$

with

$$\mathcal{H}_0(nk) = \begin{pmatrix} 0 & 0 & \gamma[\kappa(n) - \mathrm{i}k] & 0 \\ 0 & 0 & 0 & \gamma[\kappa(n) + \mathrm{i}k] \\ \gamma[\kappa(n) + \mathrm{i}k] & 0 & 0 & 0 \\ 0 & \gamma[\kappa(n) - \mathrm{i}k] & 0 & 0 \end{pmatrix}, \tag{2.10}$$

and

$$\varepsilon_{snk} = s\gamma\sqrt{\kappa(n)^2 + k^2}. \tag{2.11}$$

For an impurity localized at a carbon A site $\boldsymbol{r}_j$, we have[32]

$$V(\boldsymbol{r}) = V_j \delta(\boldsymbol{r} - \boldsymbol{r}_j), \tag{2.12}$$

with

$$V_j = \begin{pmatrix} u_j \Phi_j^A & 0 \\ 0 & 0 \end{pmatrix}, \tag{2.13}$$

where

$$\Phi_j^A = \begin{pmatrix} 1 & \mathrm{e}^{\mathrm{i}\phi_j^A} \\ \mathrm{e}^{-\mathrm{i}\phi_j^A} & 1 \end{pmatrix}, \tag{2.14}$$

with

$$\phi_j^A = (\boldsymbol{K}' - \boldsymbol{K}) \cdot \boldsymbol{r}_j + \eta. \tag{2.15}$$

Here, η is the chiral angle shown in Fig. 1. Define further a vector $\boldsymbol{a}_j$ as

$$\boldsymbol{a}_j = \begin{pmatrix} a_{jK} \\ a_{jK'} \end{pmatrix} = \frac{1}{\sqrt{2}} \begin{pmatrix} \mathrm{e}^{\mathrm{i}\phi_j^A/2} \\ \mathrm{e}^{-\mathrm{i}\phi_j^A/2} \end{pmatrix}, \tag{2.16}$$

which satisfies

$$(\boldsymbol{a}_j, \boldsymbol{a}_j) = \boldsymbol{a}_j^+ \boldsymbol{a}_j = 1, \quad a_{jK'} = a_{jK}^*. \tag{2.17}$$

Then, we have

$$\Phi_j^A = 2\boldsymbol{a}_j \boldsymbol{a}_j^+. \tag{2.18}$$

For an impurity localized at a carbon B site $\boldsymbol{r}_j$, we

have

$$V_j = \begin{pmatrix} 0 & 0 \\ 0 & u_j \Phi_j^B \end{pmatrix}, \tag{2.19}$$

where

$$\Phi_j^B = \begin{pmatrix} 1 & \mathrm{e}^{\mathrm{i}\phi_j^B} \\ \mathrm{e}^{-\mathrm{i}\phi_j^B} & 1 \end{pmatrix}, \tag{2.20}$$

with

$$\phi_j^B = (\boldsymbol{K}'-\boldsymbol{K})\cdot\boldsymbol{r}_j - \eta + \frac{\pi}{3}. \tag{2.21}$$

In terms of a vector $\boldsymbol{b}_j$ defined as

$$\boldsymbol{b}_j = \begin{pmatrix} b_{jK} \\ b_{jK'} \end{pmatrix} = \frac{1}{\sqrt{2}} \begin{pmatrix} \mathrm{e}^{\mathrm{i}\phi_j^B/2} \\ \mathrm{e}^{-\mathrm{i}\phi_j^B/2} \end{pmatrix}, \tag{2.22}$$

we have

$$\Phi_j^B = 2\boldsymbol{b}_j\boldsymbol{b}_j^+. \tag{2.23}$$

2.2 Scattering matrix

In terms of a T matrix defined by

$$T = V + V\frac{1}{\varepsilon-\mathcal{H}_0+\mathrm{i}0}V + V\frac{1}{\varepsilon-\mathcal{H}_0+\mathrm{i}0}V\frac{1}{\varepsilon-\mathcal{H}_0+\mathrm{i}0}V + \cdots, \tag{2.24}$$

the scattering matrix can be written formally as

$$S = S^{(0)} + S^{(1)}, \tag{2.25}$$

with

$$S_{\alpha\beta}^{(0)} = \delta_{\alpha\beta}, \tag{2.26}$$

and

$$S_{\alpha\beta}^{(1)} = -\mathrm{i}\frac{A}{\hbar\sqrt{|v_\alpha v_\beta|}}T_{\alpha\beta}, \tag{2.27}$$

where v_α and v_β are the velocity of channels α and β.

The matrix element is written as

$$(\alpha|V_j|\beta) = \boldsymbol{f}_\alpha^+ V_j \boldsymbol{f}_\beta \frac{1}{AL}\exp[-\mathrm{i}(\kappa_\alpha-\kappa_\beta)x_j - \mathrm{i}(k_\alpha-k_\beta)y_j], \tag{2.28}$$

where (x_j, y_j) is the position of the impurity, $\boldsymbol{f}_\alpha$ is the eigenvector for the state α with energy ε_α, wave vector in the axis direction k_α, and that in the circumference direction $\kappa_\alpha = \kappa(n_\alpha) \equiv (2\pi/L)n_\alpha$ with integer n_α. The T matrix is expanded as

$$T = T^{(1)} + T^{(2)} + T^{(3)} + \cdots, \tag{2.29}$$

with

$$(\alpha|T^{(1)}|\beta) = \sum_j \boldsymbol{f}_\alpha^+ \frac{1}{AL} V_j \boldsymbol{f}_\beta \exp[-\mathrm{i}\kappa_{\alpha\beta}x_j - \mathrm{i}k_{\alpha\beta}y_j], \tag{2.30}$$

$$(\alpha|T^{(2)}|\beta) = \sum_\gamma \sum_j \boldsymbol{f}_\alpha^+ \frac{1}{AL} V_j \boldsymbol{f}_\gamma \exp[-\mathrm{i}\kappa_{\alpha\gamma}x_j - \mathrm{i}k_{\alpha\gamma}y_j] \times \frac{1}{\varepsilon-\varepsilon_\gamma+\mathrm{i}0} \sum_{j'} \boldsymbol{f}_\gamma^+ \frac{1}{AL} V_{j'} \boldsymbol{f}_\beta \exp[-\mathrm{i}\kappa_{\gamma\beta}x_{j'} - \mathrm{i}k_{\gamma\beta}y_{j'}], \tag{2.31}$$

$$(\alpha|T^{(3)}|\beta) = \sum_{\gamma\gamma'} \sum_j \boldsymbol{f}_\alpha^+ \frac{1}{AL} V_j \boldsymbol{f}_\gamma \exp[-\mathrm{i}\kappa_{\alpha\gamma}x_j - \mathrm{i}k_{\alpha\gamma}y_j] \times \frac{1}{\varepsilon-\varepsilon_\gamma+\mathrm{i}0} \sum_{j'} \boldsymbol{f}_\gamma^+ \frac{1}{AL} V_{j'} \boldsymbol{f}_{\gamma'} \exp[-\mathrm{i}\kappa_{\gamma\gamma'}x_{j'} - \mathrm{i}k_{\gamma\gamma'}y_{j'}] \times \frac{1}{\varepsilon-\varepsilon_{\gamma'}+\mathrm{i}0} \sum_{j''} \boldsymbol{f}_{\gamma'}^+ \frac{1}{AL} V_{j''} \boldsymbol{f}_\beta \exp[-\mathrm{i}\kappa_{\gamma'\beta}x_{j''} - \mathrm{i}k_{\gamma'\beta}y_{j''}], \tag{2.32}$$

where $\kappa_{\alpha\beta} \equiv \kappa_\alpha - \kappa_\beta$, $k_{\alpha\beta} \equiv k_\alpha - k_\beta$, etc. In the lowest order Born approximation, the T matrix is given by eq. (2.30), which shows that the effective potential is essentially given by the sum of the potential of each impurity.

We note the relation:

$$\sum_\gamma \boldsymbol{f}_\gamma \frac{1}{\varepsilon-\varepsilon_\gamma+\mathrm{i}0}\boldsymbol{f}_\gamma^+ = \sum_{nk} \big[\varepsilon - \mathcal{H}_0(nk) + \mathrm{i}0\big]^{-1}. \tag{2.33}$$

Then, the second order term becomes

$$\sum_{jj'} \boldsymbol{f}_\alpha^+ \frac{1}{AL} V_j G_{jj'}(\varepsilon+\mathrm{i}0) \frac{1}{AL} V_{j'} \boldsymbol{f}_\beta \times \exp(-\mathrm{i}\kappa_\alpha x_j - \mathrm{i}k_\alpha y_j)\exp(\mathrm{i}\kappa_\beta x_{j'} + \mathrm{i}k_\beta y_{j'}), \tag{2.34}$$

where

$$G_{jj'}(\varepsilon+\mathrm{i}0) \equiv G(\boldsymbol{r}_j - \boldsymbol{r}_{j'}, \varepsilon+\mathrm{i}0) = \sum_{nk} \big[\varepsilon - \mathcal{H}_0(nk) + \mathrm{i}0\big]^{-1} \exp[\mathrm{i}\kappa(n)x_{jj'} + \mathrm{i}ky_{jj'}], \tag{2.35}$$

with

$$x_{jj'} = x_j - x_{j'}, \quad y_{jj'} = y_j - y_{j'}. \tag{2.36}$$

Similarly, the third order term is given by

$$\sum_{jj'j''} \boldsymbol{f}_\alpha^+ \frac{1}{AL} V_j G_{jj''}(\varepsilon+\mathrm{i}0) \frac{1}{AL} V_{j''} G_{j''j'}(\varepsilon+\mathrm{i}0) \frac{1}{AL} V_{j'} \boldsymbol{f}_\beta \times \exp(-\mathrm{i}\kappa_\alpha x_j - \mathrm{i}k_\alpha y_j)\exp(\mathrm{i}\kappa_\beta x_{j'} + \mathrm{i}k_\beta y_{j'}). \tag{2.37}$$

By repeating similar procedures up to an infinite order, we obtain the T matrix

$$(\alpha|T|\beta) = \sum_{ij} \boldsymbol{f}_\alpha^+ T_{ij} \boldsymbol{f}_\beta \exp(-\mathrm{i}\kappa_\alpha x_i - \mathrm{i}k_\alpha y_i) \times \exp(\mathrm{i}\kappa_\beta x_j + \mathrm{i}k_\beta y_j), \tag{2.38}$$

where

$$T_{ij} = \Big[\Big(1 - \frac{1}{AL}VG(\varepsilon+\mathrm{i}0)\Big)^{-1}\frac{1}{AL}V\Big]_{ij}, \tag{2.39}$$

with $V_{jj'} = V_j\delta_{jj'}$.

The equation for T_{ij} is given by

$$T_{ij} = \frac{1}{AL}V_i\delta_{ij} + \frac{1}{AL}V_i\sum_k G(\boldsymbol{r}_i - \boldsymbol{r}_k, \varepsilon+\mathrm{i}0)T_{kj}. \tag{2.40}$$

Effects of multiple scattering from a single impurity can exactly be taken into account by replacing eq. (2.40) by

$$T_{ij} = \frac{1}{AL}V_i\delta_{ij} + \frac{1}{AL}V_iG(0, \varepsilon+\mathrm{i}0)T_{ij} + \frac{1}{AL}V_i\sum_{k\neq i} G(\boldsymbol{r}_i - \boldsymbol{r}_k, \varepsilon+\mathrm{i}0)T_{kj}. \tag{2.41}$$

We then have

$$T_{ij} = \frac{1}{AL}\tilde{V}_i\delta_{ij} + \frac{1}{AL}\tilde{V}_i\sum_{k\neq i} G(\boldsymbol{r}_i - \boldsymbol{r}_k, \varepsilon+\mathrm{i}0)T_{kj}, \tag{2.42}$$

with

$$\tilde{V}_i = \Big[1 - \frac{1}{AL}V_iG(0, \varepsilon+\mathrm{i}0)\Big]^{-1}V_i. \tag{2.43}$$

In the following, we shall confine ourselves to the

case that

$$-\frac{2\pi\gamma}{L} < \varepsilon < \frac{2\pi\gamma}{L}. \tag{2.44}$$

For this energy range, the eigen vectors are given by

$$\boldsymbol{f}_{K\pm} = \frac{1}{\sqrt{2}} \begin{pmatrix} 1 \\ 0 \\ \pm\mathrm{i} \\ 0 \end{pmatrix}, \quad \boldsymbol{f}_{K'\pm} = \frac{1}{\sqrt{2}} \begin{pmatrix} 0 \\ 1 \\ 0 \\ \mp\mathrm{i} \end{pmatrix}, \tag{2.45}$$

and the velocity is given by $|v| = \gamma/\hbar$. We can write the scattering matrix as

$$S = \begin{pmatrix} r_{KK} & r_{KK'} & t'_{KK} & t'_{KK'} \\ r_{K'K} & r_{K'K'} & t'_{K'K} & t'_{K'K'} \\ t_{KK} & t_{KK'} & r'_{KK} & r'_{KK'} \\ t_{K'K} & t_{K'K'} & r'_{K'K} & r'_{K'K'} \end{pmatrix}, \tag{2.46}$$

where t's and r's are transmission and reflection coefficients, respectively. When all impurities are localized in a region smaller than the circumference and $|\varepsilon| \ll 2\pi\gamma/L$, in particular, eq. (2.38) can be replaced by

$$(\alpha|T|\beta) = \boldsymbol{f}_\alpha^+ T_\mathrm{S} \boldsymbol{f}_\beta \exp[-\mathrm{i}(\kappa_\alpha - \kappa_\beta)x_0 - \mathrm{i}(k_\alpha - k_\beta)y_0], \tag{2.47}$$

with

$$T_\mathrm{S} = \sum_{ij} T_{ij}, \tag{2.48}$$

where $\boldsymbol{r}_0 = (x_0, y_0)$ is the center-of-mass of all the impurities.

2.3 Green's functions

The Green's function is explicitly given by

$$G(x,y,\varepsilon+\mathrm{i}0) = \frac{A}{2\pi} \int \mathrm{d}k \sum_n \frac{f_\mathrm{c}[\kappa(n),k]\, \mathrm{e}^{\mathrm{i}\kappa(n)x + \mathrm{i}ky}}{(\varepsilon+\mathrm{i}0)^2 - \gamma^2[\kappa(n)^2+k^2]} \times \begin{pmatrix} \varepsilon & 0 & \gamma[\kappa(n)-\mathrm{i}k] & 0 \\ 0 & \varepsilon & 0 & \gamma[\kappa(n)+\mathrm{i}k] \\ \gamma[\kappa(n)+\mathrm{i}k] & 0 & \varepsilon & 0 \\ 0 & \gamma[\kappa(n)-\mathrm{i}k] & 0 & \varepsilon \end{pmatrix}, \tag{2.49}$$

where we have introduced a cutoff function $f_\mathrm{c}[\kappa(n),k]$ defined by

$$f_\mathrm{c}[\kappa(n),k] = \frac{k_\mathrm{c}^2}{k^2+\kappa(n)^2+k_\mathrm{c}^2}, \tag{2.50}$$

in order to extract the contribution from states in the vicinity of the Fermi level. The cutoff wave vector k_c is determined by the condition that the cutoff wave length $2\pi/k_\mathrm{c}$ should be comparable to the lattice constant a, i.e., $2\pi/k_\mathrm{c} \approx a$. We introduce a cutoff integer n_c by $k_\mathrm{c} = 2\pi n_\mathrm{c}/L$, i.e., $\kappa(n_\mathrm{c}) \approx k_\mathrm{c}$ or $n_\mathrm{c} \approx L/a$. The Green's function is written as

$$G = \frac{-\mathrm{i}A}{2\gamma} \begin{pmatrix} g_0 & 0 & g_1 & 0 \\ 0 & g_0 & 0 & \bar{g}_1 \\ \bar{g}_1 & 0 & g_0 & 0 \\ 0 & g_1 & 0 & g_0 \end{pmatrix}, \tag{2.51}$$

where

$$g_0(x,y) = \frac{\mathrm{i}\gamma}{\pi} \int \mathrm{d}k \sum_n f_\mathrm{c}[\kappa(n),k] \frac{\varepsilon \mathrm{e}^{\mathrm{i}\kappa(n)x + \mathrm{i}ky}}{(\varepsilon+\mathrm{i}0)^2 - \gamma^2[\kappa(n)^2+k^2]},$$
$$g_1(x,y) = \frac{\mathrm{i}\gamma}{\pi} \int \mathrm{d}k \sum_n f_\mathrm{c}[\kappa(n),k] \frac{\gamma[\kappa(n)-\mathrm{i}k]\mathrm{e}^{\mathrm{i}\kappa(n)x + \mathrm{i}ky}}{(\varepsilon+\mathrm{i}0)^2 - \gamma^2[\kappa(n)^2+k^2]}, \tag{2.52}$$

and $\bar{g}_1(x,y) = g_1(x,-y)$. We immediately see that

$$g_0(-x,y) = g_0(x,-y) = g_0(-x,-y) = g_0(x,y), \quad g_1(-x,-y) = -g_1(x,y), \tag{2.53}$$

which leads to $g_1(0,0) = 0$.

The off-diagonal Green's function appears only between matrix elements of impurities and therefore in the form

$$\boldsymbol{a}_i^+ \begin{pmatrix} g_1(\boldsymbol{r}_{ij}) & 0 \\ 0 & \bar{g}_1(\boldsymbol{r}_{ij}) \end{pmatrix} \boldsymbol{b}_j = (\boldsymbol{a}_i, \boldsymbol{b}_j)\, \tilde{g}_{ij}^{AB}, \tag{2.54}$$

with $\boldsymbol{r}_{ij} = \boldsymbol{r}_i - \boldsymbol{r}_j$, where

$$\tilde{g}_{ij}^{AB} = \frac{1}{2}\big[g_1(\boldsymbol{r}_{ij})\mathrm{e}^{-\mathrm{i}(\phi_i^A - \phi_j^B)/2} + \bar{g}_1(\boldsymbol{r}_{ij})\mathrm{e}^{\mathrm{i}(\phi_i^A - \phi_j^B)/2}\big] \times (\boldsymbol{a}_i, \boldsymbol{b}_j)^{-1}, \tag{2.55}$$

and $(\boldsymbol{a}_i, \boldsymbol{b}_j) = \boldsymbol{a}_i^+ \boldsymbol{b}_j$. This means that we can always use $\tilde{g}_{ij}^{AB}$ for the off-diagonal Green's function describing the propagation from a B site at $\boldsymbol{r}_j$ to an A site at $\boldsymbol{r}_i$. It should be noted that $(\boldsymbol{a}_i, \boldsymbol{b}_j) = \boldsymbol{a}^+\boldsymbol{b}$ is real.

In the energy range (2.44), we have

$$g_0(x,y) = \mathrm{e}^{\mathrm{i}(\epsilon/\gamma)|y|} - 2\mathrm{i}\varepsilon \sum_{n=1}^{\infty} \cos[\kappa(n)x] \Big(\frac{\exp[-\sqrt{\kappa(n)^2 - (\varepsilon/\gamma)^2}\,|y|]}{\sqrt{\gamma^2\kappa(n)^2 - \varepsilon^2}} - \frac{\exp[-\sqrt{\kappa(n)^2 + k_\mathrm{c}^2}\,|y|]}{\sqrt{\gamma^2\kappa(n)^2 + \gamma^2 k_\mathrm{c}^2}} \Big), \tag{2.56}$$

and

$$g_1(x,y) = -\mathrm{i}\,\mathrm{sgn}(y)\big[\mathrm{e}^{\mathrm{i}(\epsilon/\gamma)|y|} - \mathrm{e}^{-k_\mathrm{c}|y|}\big] + 2\sum_{n=1}^{\infty} \Big(\Big[\frac{\kappa(n)\sin[\kappa(n)x]}{\sqrt{\kappa(n)^2 - (\epsilon/\gamma)^2}} - \mathrm{i}\,\mathrm{sgn}(y)\cos[\kappa(n)x] \Big] \times \exp\big[-\sqrt{\kappa(n)^2 - (\epsilon/\gamma)^2}\,|y|\big] - \Big[\frac{\kappa(n)\sin[\kappa(n)x]}{\sqrt{\kappa(n)^2 + k_\mathrm{c}^2}} - \mathrm{i}\,\mathrm{sgn}(y)\cos[\kappa(n)x] \Big] \times \exp\big[-\sqrt{\kappa(n)^2 + k_\mathrm{c}^2}\,|y|\big] \Big), \tag{2.57}$$

with

$$\mathrm{sgn}(y) = \begin{cases} +1 & (y > 0)\ ; \\ 0 & (y = 0)\ ; \\ -1 & (y < 0)\ . \end{cases} \tag{2.58}$$

At $\varepsilon = 0$, in particular, we have

$$g_0(x,y) = 1, \tag{2.59}$$

and

$$g_1(x,y) = -\mathrm{i}\,\mathrm{sgn}(y)\big[1 - \mathrm{e}^{-k_\mathrm{c}|y|}\big] + 2\sum_{n=1}^{\infty} \Big(\Big[\sin[\kappa(n)x] - \mathrm{i}\,\mathrm{sgn}(y)\cos[\kappa(n)x] \Big] \exp\big[-\kappa(n)|y|\big] - \Big[\frac{\kappa(n)\sin[\kappa(n)x]}{\sqrt{\kappa(n)^2 + k_\mathrm{c}^2}} - \mathrm{i}\,\mathrm{sgn}(y)\cos[\kappa(n)x] \Big] \times \exp\big[-\sqrt{\kappa(n)^2 + k_\mathrm{c}^2}\,|y|\big] \Big). \tag{2.60}$$

The above shows that

$$\bar{g}_1(x,y) = g_1(x,y)^*, \tag{2.61}$$

and consequently

$$\tilde{g}_{ij}^{AB} = \mathrm{Re}\big[g_1(\boldsymbol{r}_{ij})\mathrm{e}^{-\mathrm{i}(\phi_i^A-\phi_j^B)/2}\big](\boldsymbol{a}_i,\boldsymbol{b}_j)^{-1}, \qquad (2.62)$$

i.e., $\tilde{g}_{ij}^{AB}$ is real as well as g_0. When $|y|\gg 2\pi/k_\mathrm{c}$, we can neglect terms containing cutoff k_c and have

$$g_1(x,y) = \frac{\cos[\pi(x+\mathrm{i}y)/L]}{\sin[\pi(x+\mathrm{i}y)/L]}. \qquad (2.63)$$

This expression is not singular at $y=0$ except when $x\sim 0$ and therefore valid in the whole (x,y) plane except in the vicinity of the origin, i.e., $|\boldsymbol{r}|\lesssim 2\pi/k_\mathrm{c}$. In particular, we have $g_1(\pm L/2,y)=0$ for $y=0$ and $g_1(x,y)\to -\mathrm{i}\,\mathrm{sgn}(y)$ for $|y|\gg L/\pi$ at $x=0$.

Figure 2 shows $G_{KA,KB}(x,y) = (-\mathrm{i}A/2\gamma)g_1(x,y)$ obtained numerically for several values of the cutoff n_c. The Green's function is singular in the vicinity of $\boldsymbol{r}=0$ as has been discussed above and the singularity is cutoff at small $r_\mathrm{c}\sim\delta L/n_\mathrm{c}$, where $\delta\sim 0.2$. This value is smaller than the cutoff distance $a\sim L/n_\mathrm{c}$, showing that the approximate expression with infinite cutoff, eq. (2.63) for $\varepsilon=0$ for example, can be used in actual calculations. For impurities localized within a distance of a few times of the lattice constant, the off-diagonal Green's function becomes extremely large. This singular behavior will be shown in §3 to be the origin of the peculiar dependence of the conductance on the difference in the number of vacancies at A and B sublattices.

Near $\varepsilon=\pm 2\pi\gamma/L$ the Green's functions diverge in proportion to $[(2\pi\gamma/L)^2-\varepsilon^2]^{-1/2}$. In fact, we have

$$g_0(x,y)\sim -\mathrm{sgn}(\varepsilon)\frac{\sqrt{2}\mathrm{i}\cos(2\pi x/L)}{\sqrt{1-|\varepsilon|(L/2\pi\gamma)}}, \qquad (2.64)$$

and

$$g_1(x,y)\sim \frac{\sqrt{2}\sin(2\pi x/L)}{\sqrt{1-|\varepsilon|(L/2\pi\gamma)}}. \qquad (2.65)$$

For a small distance, i.e., $|x/L|\ll 1$, the divergence at $\varepsilon=\pm 2\pi\gamma/L$ is much stronger for the diagonal Green's function than for the off-diagonal Green' function, i.e., $|g_0^{-1}g_1|\ll 1$ near $\varepsilon=\pm 2\pi\gamma/L$ in contrast to $|g_0^{-1}g_1|\gg 1$ in the other energy range. The energy corresponding to this crossover approaches $\varepsilon=2\pi\gamma/L$ with the increase of the circumference. This shows that a singular energy dependence appears in the conductance for closely spaced impurities located at both A and B sublattices in the vicinity of $\varepsilon=\pm 2\pi\gamma/L$, as will be demonstrated in §3 and §4.

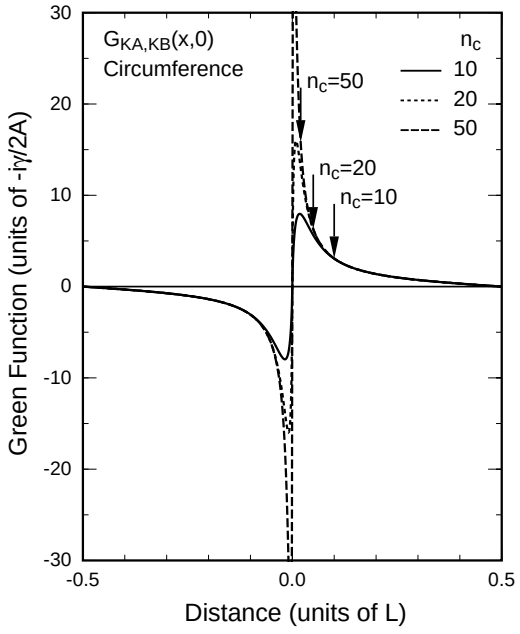

(a)

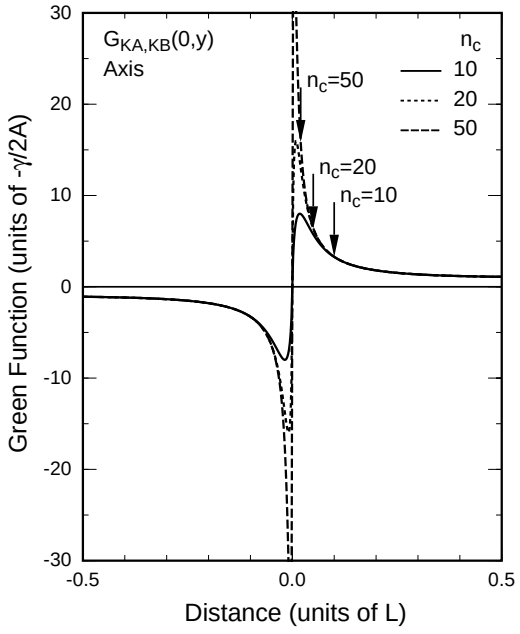

(b)

Fig. 2 The off-diagonal Green's function for (a) $y=0$ and for (b) $x=0$ for several values of n_c. The vertical arrows show the value of the cutoff distance L/n_c.

At $\boldsymbol{r}=0$, the diagonal Green's function is written as

$$g_0(0,0) = 1 - \mathrm{i}g_0''(\varepsilon), \qquad (2.66)$$

with

$$g_0''(\varepsilon) = 2\varepsilon\sum_{n=1}^{\infty}\Big(\frac{1}{\sqrt{\gamma^2\kappa(n)^2-\varepsilon^2}}-\frac{1}{\sqrt{\gamma^2\kappa(n)^2+\gamma^2k_\mathrm{c}^2}}\Big). \qquad (2.67)$$

The imaginary part $g_0''(\varepsilon)$ is a monotonic function of ε in the energy range (2.44) and behaves as

$$g_0''(\varepsilon)\approx 2\chi\frac{\epsilon L}{2\pi\gamma}, \qquad (2.68)$$

with

$$\chi=\sum_{n=1}^{\infty}\Big(\frac{1}{n}-\frac{1}{\sqrt{n^2+n_{\rm c}^2}}\Big)\approx\ln n_{\rm c}, \tag{2.69}$$

for $|\varepsilon(L/2\pi\gamma)|\ll 1$ and

$$g_0''(\varepsilon)\approx\mathrm{sgn}(\varepsilon)\sqrt{\frac{2}{1-|\varepsilon|(L/2\pi\gamma)}}, \tag{2.70}$$

for $\varepsilon\sim\pm 2\pi\gamma/L$.

2.4 T matrix

The Green's function becomes diagonal for $\boldsymbol{r}=0$ and therefore the renormalized impurity potential for an A site, for example, by taking into account multiple scattering, becomes

$$u_j\Phi_j^A\to\Big(1-\frac{1}{AL}u_j\Phi_j^A\frac{-\mathrm{i}A}{2\gamma}g_0\Big)^{-1}u_j\Phi_j^A=\frac{\gamma L}{\mathrm{i}g_0}\zeta_j\Phi_j^A, \tag{2.71}$$

where $g_0\equiv g_0(0,\varepsilon+\mathrm{i}0)$ for simplicity, use has been made of $\big(\Phi_j^A\big)^n=2^n\Phi_j^A$, which follows immediately from eq. (2.18), and $\zeta_j=[1+(2\mathrm{i}\tilde{u}_jg_0)^{-1}]^{-1}$ with $\tilde{u}_j=u_j/2\gamma L$. This shows that due to the multiple scattering from a single impurity the potential strength u_j is renormalized into $\zeta_j\gamma L/\mathrm{i}g_0$.

When impurities are separated into those at A and B sublattices, we have

$$\begin{aligned}T_{ij}^{AA}=&\frac{1}{AL}\frac{\gamma L}{\mathrm{i}g_0}\zeta_i\Phi_i^A\delta_{ij}\\&+\frac{1}{AL}\frac{\gamma L}{\mathrm{i}g_0}\zeta_i\Phi_i^A\sum_{k\neq i,\,k\in A}\frac{-\mathrm{i}A}{2\gamma}g_0(\boldsymbol{r}_{ik})T_{kj}^{AA}\\&+\frac{1}{AL}\frac{\gamma L}{\mathrm{i}g_0}\zeta_i\Phi_i^A\sum_{k\in B}\frac{-\mathrm{i}A}{2\gamma}\tilde{g}_{ik}^{AB}T_{kj}^{BA},\end{aligned} \tag{2.72}$$

$$\begin{aligned}T_{ij}^{BA}=&\frac{1}{AL}\frac{\gamma L}{\mathrm{i}g_0}\zeta_i\Phi_i^B\sum_{k\neq i,\,k\in B}\frac{-\mathrm{i}A}{2\gamma}g_0(\boldsymbol{r}_{ik})T_{kj}^{BA}\\&+\frac{1}{AL}\frac{\gamma L}{\mathrm{i}g_0}\zeta_i\Phi_i^B\sum_{k\in A}\frac{-\mathrm{i}A}{2\gamma}\tilde{g}_{ik}^{BA}T_{kj}^{AA},\end{aligned} \tag{2.73}$$

$$\begin{aligned}T_{ij}^{BB}=&\frac{1}{AL}\frac{\gamma L}{\mathrm{i}g_0}\zeta_i\Phi_i^B\delta_{ij}\\&+\frac{1}{AL}\frac{\gamma L}{\mathrm{i}g_0}\zeta_i\Phi_i^B\sum_{k\neq i,\,k\in B}\frac{-\mathrm{i}A}{2\gamma}g_0(\boldsymbol{r}_{ik})T_{kj}^{BB}\\&+\frac{1}{AL}\frac{\gamma L}{\mathrm{i}g_0}\zeta_i\Phi_i^B\sum_{k\in A}\frac{-\mathrm{i}A}{2\gamma}\tilde{g}_{ik}^{BA}T_{kj}^{AB},\end{aligned} \tag{2.74}$$

and

$$\begin{aligned}T_{ij}^{AB}=&\frac{1}{AL}\frac{\gamma L}{\mathrm{i}g_0}\zeta_i\Phi_i^A\sum_{k\neq i,\,k\in A}\frac{-\mathrm{i}A}{2\gamma}g_0(\boldsymbol{r}_{ik})T_{kj}^{AB}\\&+\frac{1}{AL}\frac{\gamma L}{\mathrm{i}g_0}\zeta_i\Phi_i^A\sum_{k\in B}\frac{-\mathrm{i}A}{2\gamma}\tilde{g}_{ik}^{AB}T_{kj}^{BB},\end{aligned} \tag{2.75}$$

where T_{ij}^{AA}, etc. are a $(2,2)$ matrix.

In the following we shall confine ourselves to the case that the strength of all the impurities is the same and given by u, i.e., $u_j=u$. In this case, an examination of perturbation series with respect to the impurity potential reveals that the T matrices can be written as

$$\begin{aligned}T_{ij}^{AA}&=\frac{1}{AL}\frac{\gamma L}{\mathrm{i}g_0}\zeta\,2\boldsymbol{a}_i\boldsymbol{a}_j^+\,t_{ij}^{AA},\\T_{ij}^{BA}&=\frac{1}{AL}\frac{\gamma L}{\mathrm{i}g_0}\zeta\,2\boldsymbol{b}_i\boldsymbol{a}_j^+\,t_{ij}^{BA},\\T_{ij}^{BB}&=\frac{1}{AL}\frac{\gamma L}{\mathrm{i}g_0}\zeta\,2\boldsymbol{b}_i\boldsymbol{b}_j^+\,t_{ij}^{BB},\\T_{ij}^{AB}&=\frac{1}{AL}\frac{\gamma L}{\mathrm{i}g_0}\zeta\,2\boldsymbol{a}_i\boldsymbol{b}_j^+\,t_{ij}^{AB},\end{aligned} \tag{2.76}$$

where

$$\zeta=\frac{1}{1+(2\mathrm{i}\tilde{u}g_0)^{-1}},\quad\frac{\zeta}{g_0}=\frac{\mathrm{i}}{g_0''(\varepsilon)+(2\tilde{u})^{-1}+\mathrm{i}}. \tag{2.77}$$

Note that $\zeta\to 1$ in the limit $\tilde{u}=u/2\gamma L\to\infty$. Then, we have

$$\begin{aligned}t_{ij}^{AA}=&\delta_{ij}-\zeta g_0^{-1}\sum_{k\neq i,\,k\in A}g_0(\boldsymbol{r}_{ik})\boldsymbol{a}_i^+\boldsymbol{a}_kt_{kj}^{AA}\\&-\zeta g_0^{-1}\sum_{k\in B}\tilde{g}_{ik}^{AB}\boldsymbol{a}_i^+\boldsymbol{b}_kt_{kj}^{BA},\\t_{ij}^{BA}=&-\zeta g_0^{-1}\sum_{k\neq i,\,k\in B}g_0(\boldsymbol{r}_{ik})\boldsymbol{b}_i^+\boldsymbol{b}_kt_{kj}^{BA}\\&-\zeta g_0^{-1}\sum_{k\in A}\tilde{g}_{ik}^{BA}\boldsymbol{b}_i^+\boldsymbol{a}_kt_{kj}^{AA},\end{aligned} \tag{2.78}$$

and

$$\begin{aligned}t_{ij}^{BB}=&\delta_{ij}-\zeta g_0^{-1}\sum_{k\neq i,\,k\in B}g_0(\boldsymbol{r}_{ik})\boldsymbol{b}_i^+\boldsymbol{b}_kt_{kj}^{BB}\\&-\zeta g_0^{-1}\sum_{k\in A}\tilde{g}_{ik}^{BA}\boldsymbol{b}_i^+\boldsymbol{a}_kt_{kj}^{AB},\\t_{ij}^{AB}=&-\zeta g_0^{-1}\sum_{k\neq i,\,k\in A}g_0(\boldsymbol{r}_{ik})\boldsymbol{a}_i^+\boldsymbol{a}_kt_{kj}^{AB}\\&-\zeta g_0^{-1}\sum_{k\in B}\tilde{g}_{ik}^{AB}\boldsymbol{a}_i^+\boldsymbol{b}_kt_{kj}^{BB}.\end{aligned} \tag{2.79}$$

In the case of a finite number of impurities, these linear equations can be solved numerically and the T matrix can be calculated explicitly.

In the following analytical treatment, we shall confine ourselves further to the case that impurities are located in an area with size much smaller than the circumference length. In this case, we can make the replacement $g_0(\boldsymbol{r}_{ik})\to g_0$ and the above set of equations is further reduced to

$$\begin{aligned}t_{ij}^{AA}&=\delta_{ij}-\zeta\sum_{k\neq i,\,k\in A}\boldsymbol{a}_i^+\boldsymbol{a}_kt_{kj}^{AA}-\zeta g_0^{-1}\sum_{k\in B}\tilde{g}_{ik}^{AB}\boldsymbol{a}_i^+\boldsymbol{b}_kt_{kj}^{BA},\\t_{ij}^{BA}&=-\zeta\sum_{k\neq i,\,k\in B}\boldsymbol{b}_i^+\boldsymbol{b}_kt_{kj}^{BA}-\zeta g_0^{-1}\sum_{k\in A}\tilde{g}_{ik}^{BA}\boldsymbol{b}_i^+\boldsymbol{a}_kt_{kj}^{AA},\\t_{ij}^{BB}&=\delta_{ij}-\zeta\sum_{k\neq i,\,k\in B}\boldsymbol{b}_i^+\boldsymbol{b}_kt_{kj}^{BB}-\zeta g_0^{-1}\sum_{k\in A}\tilde{g}_{ik}^{BA}\boldsymbol{b}_i^+\boldsymbol{a}_kt_{kj}^{AB},\\t_{ij}^{AB}&=-\zeta\sum_{k\neq i,\,k\in A}\boldsymbol{a}_i^+\boldsymbol{a}_kt_{kj}^{AB}-\zeta g_0^{-1}\sum_{k\in B}\tilde{g}_{ik}^{AB}\boldsymbol{a}_i^+\boldsymbol{b}_kt_{kj}^{BB}.\end{aligned} \tag{2.80}$$

Here, we can use eq. (2.62) for $\tilde{g}^{AB}$ and $\tilde{g}^{BA}$ because the phase factor $\exp(\mathrm{i}\varepsilon|y_{ik}|/\gamma)$ can be replaced by unity when $|y|\ll L$ and the energy is in the range (2.44). Further,

we can use eq. (2.47) and we just need the sum of T_{ij}.

Define the following matrices:

$$\begin{aligned} &t^{AA}=(t_{ij}^{AA}), \quad t^{BA}=(t_{ij}^{BA}),\\ &t^{BB}=(t_{ij}^{BB}), \quad t^{AB}=(t_{ij}^{AB}),\\ &A=(A_{ij}), \quad B=(B_{ij}),\\ &\Gamma^{AB}=(\Gamma_{ij}^{AB}), \quad \Gamma^{BA}=(\Gamma_{ij}^{BA}), \end{aligned} \tag{2.81}$$

with

$$\begin{aligned} &A_{ij}=\boldsymbol{a}_i^+\boldsymbol{a}_j, \quad B_{ij}=\boldsymbol{b}_i^+\boldsymbol{b}_j,\\ &\Gamma_{ij}^{AB}=\tilde{g}_{ij}^{AB}\boldsymbol{a}_i^+\boldsymbol{b}_j, \quad \Gamma_{ij}^{BA}=\tilde{g}_{ij}^{BA}\boldsymbol{b}_i^+\boldsymbol{a}_j. \end{aligned} \tag{2.82}$$

Let N_A be the number of impurities at A sites and N_B that at B sites. Then, t^{AA} and A are an (N_A, N_A) matrix, t^{BB} and B are an (N_B, N_B) matrix, t^{BA} and Γ^{BA} are an (N_B, N_A) matrix, and t^{AB} and Γ^{AB} are an (N_A, N_B) matrix. We have

$$\begin{aligned} &(1-\zeta+\zeta A)t^{AA}=1-\zeta g_0^{-1}\Gamma^{AB}t^{BA},\\ &(1-\zeta+\zeta B)t^{BB}=1-\zeta g_0^{-1}\Gamma^{BA}t^{AB},\\ &(1-\zeta+\zeta B)t^{BA}=-\zeta g_0^{-1}\Gamma^{BA}t^{AA},\\ &(1-\zeta+\zeta A)t^{AB}=-\zeta g_0^{-1}\Gamma^{AB}t^{BB}. \end{aligned} \tag{2.83}$$

It should be pointed out that

$$A=(\boldsymbol{a}_1\,\boldsymbol{a}_2\,\cdots\,\boldsymbol{a}_{N_A})^+(\boldsymbol{a}_1\,\boldsymbol{a}_2\,\cdots\,\boldsymbol{a}_{N_A}), \tag{2.84}$$

$$B=(\boldsymbol{b}_1\,\boldsymbol{b}_2\,\cdots\,\boldsymbol{b}_{N_B})^+(\boldsymbol{b}_1\,\boldsymbol{b}_2\,\ldots\,\boldsymbol{b}_{N_B}). \tag{2.85}$$

Further, both A and B are real symmetric matrices.

The sum of T_{ij} can be written in general as

$$T_{\rm S}=\begin{pmatrix} T^{AA} & T^{AB}\\ T^{BA} & T^{BB}\end{pmatrix}, \tag{2.86}$$

where T^{AA}, T^{AB}, T^{BA}, and T^{BB} are $(2,2)$ matrices, given by

$$\begin{aligned} &T^{AA}=\begin{pmatrix} T_{KK}^{AA} & T_{KK'}^{AA}\\ T_{K'K}^{AA} & T_{K'K'}^{AA}\end{pmatrix}, \quad T^{AB}=\begin{pmatrix} T_{KK}^{AB} & T_{KK'}^{AB}\\ T_{K'K}^{AB} & T_{K'K'}^{AB}\end{pmatrix},\\ &T^{BA}=\begin{pmatrix} T_{KK}^{BA} & T_{KK'}^{BA}\\ T_{K'K}^{BA} & T_{K'K'}^{BA}\end{pmatrix}, \quad T^{BB}=\begin{pmatrix} T_{KK}^{BB} & T_{KK'}^{BB}\\ T_{K'K}^{BB} & T_{K'K'}^{BB}\end{pmatrix}. \end{aligned} \tag{2.87}$$

Then, the reflection coefficients are given by

$$\begin{aligned} r_{KK}&=-\mathrm{i}\frac{A}{2\gamma}(T_{KK}^{AA}-T_{KK}^{BB}+\mathrm{i}T_{KK}^{AB}+\mathrm{i}T_{KK}^{BA}),\\ r_{K'K'}&=-\mathrm{i}\frac{A}{2\gamma}(T_{K'K'}^{AA}-T_{K'K'}^{BB}-\mathrm{i}T_{K'K'}^{AB}-\mathrm{i}T_{K'K'}^{BA}),\\ r_{K'K}&=-\mathrm{i}\frac{A}{2\gamma}(T_{K'K}^{AA}+T_{K'K}^{BB}+\mathrm{i}T_{K'K}^{AB}-\mathrm{i}T_{K'K}^{BA}),\\ r_{KK'}&=-\mathrm{i}\frac{A}{2\gamma}(T_{KK'}^{AA}+T_{KK'}^{BB}-\mathrm{i}T_{KK'}^{AB}+\mathrm{i}T_{KK'}^{BA}), \end{aligned} \tag{2.88}$$

and the transmission coefficients are given by

$$\begin{aligned} t_{KK}&=1-\mathrm{i}\frac{A}{2\gamma}(T_{KK}^{AA}+T_{KK}^{BB}+\mathrm{i}T_{KK}^{AB}-\mathrm{i}T_{KK}^{BA}),\\ t_{K'K'}&=1-\mathrm{i}\frac{A}{2\gamma}(T_{K'K'}^{AA}+T_{K'K'}^{BB}-\mathrm{i}T_{K'K'}^{AB}+\mathrm{i}T_{K'K'}^{BA}),\\ t_{K'K}&=-\mathrm{i}\frac{A}{2\gamma}(T_{K'K}^{AA}-T_{K'K}^{BB}+\mathrm{i}T_{K'K}^{AB}+\mathrm{i}T_{K'K}^{BA}),\\ t_{KK'}&=-\mathrm{i}\frac{A}{2\gamma}(T_{KK'}^{AA}-T_{KK'}^{BB}-\mathrm{i}T_{KK'}^{AB}-\mathrm{i}T_{KK'}^{BA}). \end{aligned} \tag{2.89}$$

The similar expressions are obtained for r'_{KK}, etc. and t'_{KK}, etc.

§3. Examples

3.1 Impurities at same sublattices

Consider a single impurity with strength u at an A site $\boldsymbol{r}_j$ illustrated in Fig. 3(a). In this case, we have $t^{AA}=1$ and $t^{AB}=t^{BA}=t^{BB}=0$, which leads to $T^{AB}=T^{BA}=T^{BB}=0$ and

$$T^{AA}=\frac{1}{AL}\frac{\gamma L}{\mathrm{i}g_0}\zeta\, 2\boldsymbol{a}_j\boldsymbol{a}_j^+. \tag{3.1}$$

Explicitly, we have

$$\begin{aligned} &r_{KK}=r_{K'K'}=\frac{\zeta}{2g_0},\\ &r_{K'K}=\frac{\zeta \mathrm{e}^{-\mathrm{i}\phi_j}}{2g_0}, \quad r_{KK'}=\frac{\zeta \mathrm{e}^{\mathrm{i}\phi_j}}{2g_0},\\ &t_{KK}=t_{K'K'}=1-\frac{\zeta}{2g_0},\\ &t_{K'K}=\frac{\zeta \mathrm{e}^{-\mathrm{i}\phi_j}}{2g_0}, \quad t_{KK'}=\frac{\zeta \mathrm{e}^{\mathrm{i}\phi_j}}{2g_0}. \end{aligned} \tag{3.2}$$

Equation (2.77) shows that $\zeta/g_0=1$ when $g_0''(\varepsilon)=-1/2\tilde{u}$. In this case we have $t_{KK}=t_{K'K'}=1/2$ and $|t_{KK'}|=|t_{K'K}|=1/2$, which leads to the conductance given by $G=e^2/\pi\hbar$, i.e., a half of the ideal value $2e^2/\pi\hbar$. This means that for any impurity there exists an energy at which $G=e^2/\pi\hbar$. In the limit $\tilde{u}\to\infty$, in particular, this occurs at $\varepsilon=0$, showing that the conductance is quantized into $G=e^2/\pi\hbar$ in the case of a vacancy consisting of a single A or B site.

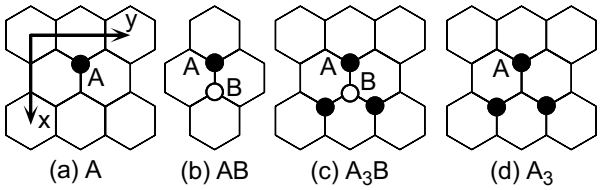

Fig. 3 Schematic illustration of vacancies in an armchair nanotube. The closed and open circles denote A and B lattice points, respectively. (a) A, (b) AB, (c) A_3B, and (d) A_3.

Next, we shall consider impurities located at two different A sites denoted as 1 and 2. The equation for t^{AA} is given by

$$(1-\zeta+\zeta A)t^{AA}=1. \tag{3.3}$$

with

$$A=(\boldsymbol{a}_1\,\boldsymbol{a}_2)^+(\boldsymbol{a}_1\,\boldsymbol{a}_2). \tag{3.4}$$

Introduce an orthogonal matrix $U=(\boldsymbol{u}_1\boldsymbol{u}_2)$ such that

$$U^+AU=\begin{pmatrix} p_1 & 0\\ 0 & p_2\end{pmatrix}, \tag{3.5}$$

i.e.,

$$A\boldsymbol{u}_j=p_j\boldsymbol{u}_j, \quad (j=1,2). \tag{3.6}$$

We choose the ordering of eigenvalues such that $p_1\geq p_2\geq$

0. Now, eq. (3.3) is solved as

$$t^{AA} = Ut'U^{+}, \tag{3.7}$$

with

$$t' = \begin{pmatrix} (1-\zeta+\zeta p_1)^{-1} & 0 \\ 0 & (1-\zeta+\zeta p_2)^{-1} \end{pmatrix}. \tag{3.8}$$

Introduce two vectors $\boldsymbol{a}'_1$ and $\boldsymbol{a}'_2$ through

$$\boldsymbol{a}'_1 = (\boldsymbol{a}_1\, \boldsymbol{a}_2)\boldsymbol{u}_1, \quad \boldsymbol{a}'_2 = (\boldsymbol{a}_1\, \boldsymbol{a}_2)\boldsymbol{u}_2, \tag{3.9}$$

Then, obviously we have

$$(\boldsymbol{a}'_1, \boldsymbol{a}'_1) = p_1, \quad (\boldsymbol{a}'_2, \boldsymbol{a}'_2) = p_2, \quad (\boldsymbol{a}'_1, \boldsymbol{a}'_2) = 0. \tag{3.10}$$

Further, the T matrix becomes

$$\begin{aligned} T_{\mathrm{S}}^{AA} &= \frac{1}{AL}\frac{\gamma L}{\mathrm{i}g_0}\zeta \sum_{i,j} t_{ij}^{AA}\, 2\boldsymbol{a}_i\boldsymbol{a}_j^{+} \\ &= \frac{1}{AL}\frac{\gamma L}{\mathrm{i}g_0}\zeta\Big(\frac{2\boldsymbol{a}'_1\boldsymbol{a}'^{+}_1}{1-\zeta+\zeta p_1} + \frac{2\boldsymbol{a}'_2\boldsymbol{a}'^{+}_2}{1-\zeta+\zeta p_2}\Big). \end{aligned} \tag{3.11}$$

First, we consider the case $\boldsymbol{a}_1 \neq \boldsymbol{a}_2$. In this case we have $p_1 \geq p_2 > 0$. Define

$$\tilde{\boldsymbol{a}}_1 = p_1^{-1/2}\boldsymbol{a}'_1, \quad \tilde{\boldsymbol{a}}_2 = p_2^{-1/2}\boldsymbol{a}'_2. \tag{3.12}$$

Then, because $\boldsymbol{u}_1$ and $\boldsymbol{u}_2$ are real, $\tilde{\boldsymbol{a}}_1$ and $\tilde{\boldsymbol{a}}_2$ can be written as

$$\tilde{\boldsymbol{a}}_j = \frac{1}{\sqrt{2}}\begin{pmatrix} \mathrm{e}^{\mathrm{i}\tilde{\phi}_j} \\ \mathrm{e}^{-\mathrm{i}\tilde{\phi}_j} \end{pmatrix}. \tag{3.13}$$

Further, the orthogonality between $\tilde{\boldsymbol{a}}_j$ leads to

$$\tilde{\phi}_1 - \tilde{\phi}_2 = \pm\pi + 2n\pi, \tag{3.14}$$

with n being an integer. Finally, the T matrix becomes

$$T_S^{AA} = \frac{1}{AL}\frac{\gamma L}{\mathrm{i}g_0}\zeta\Big(\frac{2p_1\tilde{\boldsymbol{a}}_1\tilde{\boldsymbol{a}}_1^{+}}{1-\zeta+\zeta p_1} + \frac{2p_2\tilde{\boldsymbol{a}}_2\tilde{\boldsymbol{a}}_2^{+}}{1-\zeta+\zeta p_2}\Big). \tag{3.15}$$

In the limit of a strong potential, i.e., $\tilde{u} \to \infty$ or $\zeta \to 1$, we have

$$T_S^{AA} = \frac{1}{AL}\frac{\gamma L}{\mathrm{i}g_0}\big(2\tilde{\boldsymbol{a}}_1\tilde{\boldsymbol{a}}_1^{+} + 2\tilde{\boldsymbol{a}}_2\tilde{\boldsymbol{a}}_2^{+}\big) = \frac{1}{AL}\frac{\gamma L}{\mathrm{i}g_0}\begin{pmatrix} 1 & 0 \\ 0 & 1 \end{pmatrix}, \tag{3.16}$$

where use has been made of eq. (3.14). At $\varepsilon = 0$, i.e., for $g_0 = 1$, the reflection coefficients become

$$r_{KK} = r_{K'K'} = -1, \quad r_{K'K} = r_{KK'} = 0, \tag{3.17}$$

and the transmission coefficients become

$$t_{KK} = t_{K'K'} = t_{K'K} = t_{KK'} = 0. \tag{3.18}$$

Therefore, the conductance vanishes identically in the limit $\tilde{u} \to \infty$.

Let $\boldsymbol{r}_j^A = (n_{aj}\boldsymbol{a}, n_{bj}\boldsymbol{b}) + \boldsymbol{r}_0^A$ be the impurity site, where $\boldsymbol{a}$ and $\boldsymbol{b}$ are the primitive lattice translation vectors shown in Fig. 1 and n_{aj} and n_{bj} are integers. When these positions satisfy the condition that $n_a + n_b = 3n$ with integer n, where $n_a = n_{a1} - n_{a2}$ and $n_b = n_{b1} - n_{b2}$, we have $\boldsymbol{a}_1 = \boldsymbol{a}_2$. In such a special case the rank of the matrix A is reduced and we have $p_1 > 0$, $p_2 = 0$, and $\boldsymbol{a}'_2 = 0$. Consequently, we have

$$T_S^{AA} = \frac{1}{AL}\frac{\gamma L}{\mathrm{i}g_0}\zeta\,\frac{2p_1\tilde{\boldsymbol{a}}_1\tilde{\boldsymbol{a}}_1^{+}}{1-\zeta+\zeta p_1}, \tag{3.19}$$

which in the limit $\tilde{u} \to \infty$ or $\zeta \to 1$ gives

$$T_S^{AA} = \frac{1}{AL}\frac{\gamma L}{\mathrm{i}g_0}\,2\tilde{\boldsymbol{a}}_1\tilde{\boldsymbol{a}}_1^{+}. \tag{3.20}$$

This result is completely same as that for a single impurity and leads to the conclusion that the conductance is quantized into a half of the ideal value, i.e., $G = e^2/\pi\hbar$.

Next, we consider the case of N ($N \geq 3$) impurities located at A sublattices. The equations for T matrices are same as eq. (3.3) except that A is now given by eq. (2.84). Introduce an orthogonal matrix $U = (\boldsymbol{u}_1\boldsymbol{u}_2\cdots\boldsymbol{u}_N)$ such that

$$A\boldsymbol{u}_j = p_j\boldsymbol{u}_j. \tag{3.21}$$

We choose the ordering of eigenvalues such that $p_1 \geq p_2 \geq \ldots \geq p_N \geq 0$. Then, the equation for t^{AA} can be solved as

$$t^{AA} = Ut'U^{+}, \tag{3.22}$$

with

$$t'_{ij} = \frac{\delta_{ij}}{1-\zeta+\zeta p_i}. \tag{3.23}$$

Introduce two-component vectors

$$\boldsymbol{a}'_j = (\boldsymbol{a}_1\, \boldsymbol{a}_2\, \cdots\, \boldsymbol{a}_N)\boldsymbol{u}_j. \tag{3.24}$$

Then we have

$$T_S^{AA} = \frac{1}{AL}\frac{\gamma L}{\mathrm{i}g_0}\zeta\sum_{i,j} t_{ij}^{AA}\, 2\boldsymbol{a}_i\boldsymbol{a}_j^{+} = \frac{1}{AL}\frac{\gamma L}{\mathrm{i}g_0}\zeta\sum_j \frac{2\boldsymbol{a}'_j\boldsymbol{a}'^{+}_j}{1-\zeta+\zeta p_j}. \tag{3.25}$$

Unless all $\boldsymbol{a}_i$'s are same, eq. (2.84) shows rank $A = 2$. Therefore, we have $p_j = 0$ and $\boldsymbol{a}'_j = 0$ for $j = 3, \ldots, N$. Introducing two vectors using eq. (3.12), we can show immediately that the T matrix is exactly same as that in the case of two impurities given by eqs. (3.15) and (3.16).

When $\boldsymbol{a}_j$'s are all equal, the rank of A is reduced further, i.e., rank $A = 1$, and consequently $p_2 = 0$ and $\boldsymbol{a}'_2 = 0$. Thus, the T matrix is exactly same as that in the case of a single impurity.

3.2 Pair of impurities: AB

We shall consider the case of a pair of an impurity at an A site $\boldsymbol{r}_i$ and an impurity at a B site $\boldsymbol{r}_j$ closely spaced with each other. We have

$$\begin{aligned} t^{AA} &= 1 - \zeta g_0^{-1}\tilde{g}_{ij}^{AB}\boldsymbol{a}_i^{+}\boldsymbol{b}_j t^{BA}, \\ t^{BA} &= -\zeta g_0^{-1}\tilde{g}_{ji}^{BA}\boldsymbol{b}_j^{+}\boldsymbol{a}_i t^{AA}, \\ t^{BB} &= 1 - \zeta g_0^{-1}\tilde{g}_{ji}^{BA}\boldsymbol{b}_j^{+}\boldsymbol{a}_i t^{AB}, \\ t^{AB} &= -\zeta g_0^{-1}\tilde{g}_{ji}^{AB}\boldsymbol{a}_j^{+}\boldsymbol{b}_i t^{BB}. \end{aligned} \tag{3.26}$$

Therefore, we have

$$\begin{aligned} t^{AA} = t^{BB} &= \frac{1}{1+(\zeta g_0^{-1}\tilde{g}_{ij}^{AB}\boldsymbol{a}_i^{+}\boldsymbol{b}_j)^2}, \\ t^{BA} = -t^{AB} &= \frac{\zeta g_0^{-1}\tilde{g}_{ij}^{AB}\boldsymbol{a}_i^{+}\boldsymbol{b}_j}{1+(\zeta g_0^{-1}\tilde{g}_{ji}^{BA}\boldsymbol{b}_j^{+}\boldsymbol{a}_i)^2}, \end{aligned} \tag{3.27}$$

where use has been made of $\tilde{g}_{ji}^{BA} = -\tilde{g}_{ij}^{AB}$.

First, we consider the case that the energy is away from the band edge of the bands $n = \pm 1$, i.e., $\pm 2\pi\gamma/L$.

In this case, we can safely assume that $|g_0| \sim 1$ and $|g_0^{-1}g_1| \propto L/a \gg 1$.

In the case of a sufficiently weak potential $|\tilde{u}| \ll 1$, for which $\zeta \approx 2\mathrm{i}\tilde{u}g_0$, we have $t^{AA} = t^{BB} \sim 1$ and $t^{BA} = -t^{AB} \sim 0$, i.e., $T^{BA} \approx T^{AB} \approx 0$ and

$$T^{AA} = \frac{1}{AL} u \Phi_i^A, \quad T^{BB} = \frac{1}{AL} u \Phi_j^B. \tag{3.28}$$

This is equivalent to the lowest Born result and shows that the A and B impurities can be described by an effective potential at a same lattice point $\mathbf{r}_j \approx \mathbf{r}_i$.

The lowest Born approximation becomes invalid when $|\zeta g_0^{-1} \tilde{g}_{ij}^{AB} \boldsymbol{a}_i^+ \boldsymbol{b}_j| \sim 1$. The off-diagonal Green's function is extremely large for impurities located at the distance of the order of the lattice constant and therefore the critical ζ is well approximated by $\zeta = 2\mathrm{i}\tilde{u}g_0$. Define $\tilde{u}_\mathrm{c}$ by

$$\frac{1}{2\tilde{u}_\mathrm{c}} = \tilde{g}_{ij}^{AB} \boldsymbol{a}_i^+ \boldsymbol{b}_j = -\tilde{g}_{ji}^{BA} \boldsymbol{b}_j^+ \boldsymbol{a}_i. \tag{3.29}$$

Then, the above condition is written as $|\tilde{u}| \sim |\tilde{u}_\mathrm{c}|$. We have $g_1(x,y) \approx (L/\pi)(x+\mathrm{i}y)^{-1} = (L/\pi d_{AB}) \exp(-\mathrm{i}\theta_{AB})$, where d_{AB} is the distance between the impurities and θ_{AB} is the direction angle from an impurity at a B site to that at an A site. Then, we have from eq. (2.62)

$$\tilde{g}_{ij}^{AB} \approx \frac{L}{\pi d_{AB}} \frac{\cos[\theta_{AB} + (\phi_i^A - \phi_j^B)/2]}{\cos[(\phi_i^A - \phi_j^B)/2]}, \tag{3.30}$$

which gives

$$\tilde{u}_\mathrm{c} = \frac{\pi d_{AB}}{2L} \frac{1}{\cos[\theta_{AB} + (\phi_i^A - \phi_j^B)/2]}. \tag{3.31}$$

Let V be a local site energy at an impurity and γ_0 be the transfer integral in the nearest-neighbor tight-binding model. Then, we have

$$u = \frac{\sqrt{3}}{2} a^2 V, \quad \gamma = \frac{\sqrt{3}}{2} \gamma_0 a, \quad \tilde{u} = \frac{1}{2} \frac{a}{L} \frac{V}{\gamma_0}. \tag{3.32}$$

Therefore, in terms of the local site energy, the critical value is given by

$$\frac{|V|}{\gamma_0} = \frac{\pi d_{AB}}{a} \frac{1}{|\cos[\theta_{AB} + (\phi_i^A - \phi_j^B)/2]|}, \tag{3.33}$$

which is of the order of unity for impurities with $d_{AB} \sim a$.

For small $\tilde{u}$, we have $\zeta \approx 2\mathrm{i}\tilde{u}g_0(1 - 2\mathrm{i}\tilde{u}g_0)$ and therefore

$$\begin{aligned} t^{AA} = t^{BB} &\approx \frac{1}{1 - (\tilde{u}/\tilde{u}_\mathrm{c})^2 + 4\mathrm{i}\tilde{u}g_0(\tilde{u}/\tilde{u}_\mathrm{c})^2}, \\ t^{BA} = -t^{AB} &\approx \frac{\mathrm{i}(\tilde{u}/\tilde{u}_\mathrm{c})}{1 - (\tilde{u}/\tilde{u}_\mathrm{c})^2 + 4\mathrm{i}\tilde{u}g_0(\tilde{u}/\tilde{u}_\mathrm{c})^2}. \end{aligned} \tag{3.34}$$

This shows that t^{AA}, etc. exhibit a resonance behavior at $\tilde{u} = \pm\tilde{u}_\mathrm{c}$. The width of the resonance is given by $\Delta\tilde{u} = 2\tilde{u}_\mathrm{c}^2 \propto (a/L)^2$ at $\varepsilon = 0$ and is quite narrow. At the resonance we have $|t^{AA}| \sim |t^{BB}| \sim |t^{BA}| \sim |t^{AB}| \sim 1$. The resonance is in agreement with that obtained in numerical tight-binding calculations.[38,34,35]

In order to see the resonance behavior at $\tilde{u} = \pm\tilde{u}_\mathrm{c}$ more explicitly, we shall consider the AB impurities in an armchair nanotube shown in Fig. 3(b). In this case we have $\theta_{AB} = \pi$ and $\phi_i^A - \phi_j^B = 0$ ($\eta = -\pi/2$), which give identically

$$r_{KK} = r_{K'K'} = t_{K'K} = t_{KK'} = 0, \tag{3.35}$$

according to eq. (2.88) and (2.89). This is a consequence of the mirror symmetry with respect to a plane containing the axis.[26,34] The other coefficients are

$$\begin{aligned} r_{KK'} &\approx \frac{-2\mathrm{i}\tilde{u}[1 - (\tilde{u}/\tilde{u}_\mathrm{c})]\mathrm{e}^{\mathrm{i}\phi_i^A}}{1 - (\tilde{u}/\tilde{u}_\mathrm{c})^2 + 4\mathrm{i}\tilde{u}g_0(\tilde{u}/\tilde{u}_\mathrm{c})^2}, \\ r_{K'K} &\approx \frac{-2\mathrm{i}\tilde{u}[1 + (\tilde{u}/\tilde{u}_\mathrm{c})]\mathrm{e}^{-\mathrm{i}\phi_i^A}}{1 - (\tilde{u}/\tilde{u}_\mathrm{c})^2 + 4\mathrm{i}\tilde{u}g_0(\tilde{u}/\tilde{u}_\mathrm{c})^2}, \\ t_{K'K'} &\approx 1 \frac{2\mathrm{i}\tilde{u}[1 - (\tilde{u}/\tilde{u}_\mathrm{c})]}{1 - (\tilde{u}/\tilde{u}_\mathrm{c})^2 + 4\mathrm{i}\tilde{u}g_0(\tilde{u}/\tilde{u}_\mathrm{c})^2}, \\ t_{KK} &\approx 1 \frac{2\mathrm{i}\tilde{u}[1 + (\tilde{u}/\tilde{u}_\mathrm{c})]}{1 - (\tilde{u}/\tilde{u}_\mathrm{c})^2 + 4\mathrm{i}\tilde{u}g_0(\tilde{u}/\tilde{u}_\mathrm{c})^2}, \end{aligned} \tag{3.36}$$

They show that for $\tilde{u} \sim |\tilde{u}_\mathrm{c}| = -\tilde{u}_\mathrm{c}$, for example, the resonance appears only in $r_{KK'}$ and $t_{K'K'}$ due to cancellation among different contributions and $|r_{KK'}| \sim 1$ and further $|t_{K'K'}| \sim 0$ at the resonance. The conductance at the resonance is given by $G = e^2/\pi\hbar$. These results explain the numerical results presented in §4 quite well.

Next, consider the case $|\tilde{u}| \gg |\tilde{u}_\mathrm{c}|$. In this case, $t^{AA} = t^{BB} \ll |t^{BA}| = |t^{AB}|$ and

$$t^{BA} = -t^{AB} \approx \frac{2\tilde{u}_\mathrm{c} g_0}{\zeta}. \tag{3.37}$$

Therefore, we have

$$\begin{aligned} r_{KK} = r_{K'K'} &= 2\tilde{u}_\mathrm{c} \sin[(\phi_i^A - \phi_j^B)/2], \\ r_{K'K} = r_{KK'}^* &= -2\mathrm{i}\tilde{u}_\mathrm{c} \exp[-\mathrm{i}(\phi_i^A + \phi_j^B)/2]. \end{aligned} \tag{3.38}$$

Therefore, the conductance becomes

$$G = \frac{2e^2}{\pi\hbar} \big[1 - 4\tilde{u}_\mathrm{c}^2 \big(1 + \sin^2[(\phi_i^A - \phi_j^B)/2]\big)\big]. \tag{3.39}$$

This shows that the deviation from the ideal conductance $2e^2/\pi\hbar$ is proportional to $(a/L)^2$ and vanishes in sufficiently thick nanotubes.

Consider the case that $\varepsilon \sim 2\pi\gamma/L$ for a strong scatterer $|\tilde{u}| \gg 1$. In this case eq. (2.77) shows $\zeta g_0^{-1} \approx \mathrm{i} g_0''(\varepsilon)^{-1} \to 0$ because $g_0''(\varepsilon) \to \infty$. Therefore, $t^{AA} = t^{BB}$ and $t^{BA} = -t^{AB}$ given by eq. (3.27) show a resonance behavior at $g_0''(\varepsilon) = |\tilde{g}_{ij}^{AB} \boldsymbol{a}_i^+ \boldsymbol{b}_j|$. The features of the resonance are same as those at $\tilde{u} = \pm\tilde{u}_\mathrm{c}$ discussed above and consequently the conductance is reduced to $G = e^2/\pi\hbar$ at the resonance. Because $|\tilde{g}_{ij}^{AB} \boldsymbol{a}_i^+ \boldsymbol{b}_j|$ is extremely large in the case $L/a \gg 1$, the resonance occurs at an energy very close to $2\pi\gamma/L$ as will be demonstrated by numerical results shown in §4.

Consider a pair of AB impurities located along a circumference direction with arbitrary distance d_{AB} in an armchair nanotube. In this case, we cannot use eqs. (3.26) or (3.27) because they are valid only in the case $d_{AB}/L \ll 1$ and we have to start with eqs. (2.78) and (2.79). When $\varepsilon = 0$ and $|\tilde{u}| \gg 1$, with the use of $g_1(x,y)$ given by eq. (2.63), the conductance is shown to be given by the simple analytical formula $G = (e^2/\pi\hbar)[1 + \cos(2\pi d_{AB}/L)]$ in agreement with numerical results obtained previously in a tight-binding model.[40] Analytic formula can be obtained for AB pairs

with a more general configuration but will not be presented here.

3.3 Impurities: $A_{N_A}B_{N_B}$

Let us consider the case of N_A impurities at A sublattice sites and N_B impurities at B sublattice sites. For simplicity, we assume that they are closely spaced from each other (within a distance of the order of a) and further consider the case of sufficiently thick nanotubes, i.e., $a/L\to 0$, in the energy range $|\varepsilon|\ll 2\pi\gamma/L$. Equation (2.83) can be rewritten as

$$\begin{aligned}
&(1-\zeta+\zeta A)t^{AA} = 1+\zeta^2 g_0^{-2}\Gamma^{AB}(1-\zeta+\zeta B)^{-1}\Gamma^{BA}t^{AA},\\
&(1-\zeta+\zeta B)t^{BB} = 1+\zeta^2 g_0^{-2}\Gamma^{BA}(1-\zeta+\zeta A)^{-1}\Gamma^{AB}t^{BB},\\
&(1-\zeta+\zeta B)t^{BA} = -\zeta g_0^{-1}\Gamma^{BA}t^{AA},\\
&(1-\zeta+\zeta A)t^{AB} = -\zeta g_0^{-1}\Gamma^{AB}t^{BB}.
\end{aligned} \tag{3.40}$$

First, we consider the case $N_A=N_B$. In this case, we have usually $\det\Gamma^{AB}\neq 0$ and $\det\Gamma^{BA}\neq 0$. Therefore, we have

$$\begin{aligned}
&t^{AA}\approx -\zeta^{-2}g_0^2(\Gamma^{BA})^{-1}(1-\zeta+\zeta B)(\Gamma^{AB})^{-1},\\
&t^{BA}\approx +\zeta^{-1}g_0(\Gamma^{AB})^{-1},\\
&t^{BB}\approx -\zeta^{-2}g_0^2(\Gamma^{AB})^{-1}(1-\zeta+\zeta A)(\Gamma^{AB})^{-1},\\
&t^{AB}\approx +\zeta^{-1}g_0(\Gamma^{BA})^{-1}.
\end{aligned} \tag{3.41}$$

These become extremely small when $a/L\ll 1$ and lead to the ideal conductance $G\approx 2e^2/\pi\hbar$.

Next, we consider the case $N_A>N_B$. In this case, the (N_B,N_B) matrix $\Gamma^{BA}(1-\zeta+\zeta A)^{-1}\Gamma^{AB}$ is usually not singular. Therefore, we have

$$\begin{aligned}
&t^{BB}\approx -\zeta^{-2}g_0^2[\Gamma^{BA}(1-\zeta+\zeta A)^{-1}\Gamma^{AB}]^{-1},\\
&t^{AB}\approx \zeta^{-1}g_0(1-\zeta-\zeta A)^{-1}\Gamma^{AB}[\Gamma^{BA}(1-\zeta+\zeta A)^{-1}\Gamma^{AB}]^{-1}.
\end{aligned} \tag{3.42}$$

These become extremely small in the limit of small a/L and can be neglected. On the other hand, the (N_A,N_A) matrix $\Gamma^{AB}(1-\zeta-\zeta B)^{-1}\Gamma^{BA}$ is always singular and its rank is usually N_B $(<N_A)$ which is the rank of Γ^{AB} and Γ^{BA}.

We introduce a set of orthogonal vectors with N_A components, $\boldsymbol{u}_j$ $(j=1,2,\ldots,N_A)$, such that

$$\begin{aligned}
&\Gamma^{BA}\boldsymbol{u}_j = 0, \qquad (1\le j\le N_A-N_B)\\
&\Gamma^{BA}\boldsymbol{u}_j \neq 0, \qquad (N_A-N_B<j\le N_A)
\end{aligned} \tag{3.43}$$

and make an orthogonal transformation

$$t^{AA}=Ut'U^+, \quad A=UA'U^+, \tag{3.44}$$

where

$$U=(\boldsymbol{u}_1\,\boldsymbol{u}_2\cdots\boldsymbol{u}_{N_A}). \tag{3.45}$$

Define two component vectors $\boldsymbol{a}'_j$ through

$$\boldsymbol{a}'_j=(\boldsymbol{a}_1\,\boldsymbol{a}_2\cdots\boldsymbol{a}_{N_A})\boldsymbol{u}_j. \tag{3.46}$$

Then, we have

$$A'=(\boldsymbol{a}'_1\,\boldsymbol{a}'_2\cdots\boldsymbol{a}'_{N_A})^+(\boldsymbol{a}'_1\,\boldsymbol{a}'_2\cdots\boldsymbol{a}'_{N_A}). \tag{3.47}$$

We have

$$(1-\zeta+\zeta A')t'=1+\zeta^2 g_0^{-2}Qt', \tag{3.48}$$

with

$$Q=U^+\Gamma^{AB}(1-\zeta-\zeta B)^{-1}\Gamma^{BA}U. \tag{3.49}$$

We separate the matrices as follows

$$t'=\begin{pmatrix} t'_0 & t'_1\\ t'_2 & t'_3\end{pmatrix},\ A'=\begin{pmatrix} A'_0 & A'_1\\ A'_2 & A'_3\end{pmatrix},\ Q=\begin{pmatrix} Q_0 & Q_1\\ Q_2 & Q_3\end{pmatrix}, \tag{3.50}$$

where t'_0, A'_0, and Q_0 are (N_A-N_B,N_A-N_B) matrices, etc. We have

$$Q_0=0, \quad Q_1=0, \quad Q_2=0, \tag{3.51}$$

and Q_3 is a matrix which is usually not singular. Then, we have

$$\begin{aligned}
&\begin{pmatrix} 1-\zeta+\zeta A'_0 & \zeta A'_1\\ \zeta A'_2 & 1-\zeta+\zeta A'_3\end{pmatrix}\begin{pmatrix} t'_0 & t'_1\\ t'_2 & t'_3\end{pmatrix}\\
&=\begin{pmatrix} 1 & 0\\ 0 & 1\end{pmatrix}+\zeta^2 g_0^{-2}\begin{pmatrix} 0 & 0\\ 0 & Q_3\end{pmatrix}\begin{pmatrix} t'_0 & t'_1\\ t'_2 & t'_3\end{pmatrix}.
\end{aligned} \tag{3.52}$$

In the limit $a/L\to 0$, matrix elements and therefore eigenvalues of Q_3 become infinitely large, i.e., $Q_3\to\infty$, we then have

$$(1-\zeta+\zeta A'_0)t'_0=1, \quad t'_1=0, \quad t'_2=0, \quad t'_3=0 \tag{3.53}$$

In the case $N_A-N_B>2$, we have usually $\operatorname{rank}A'_0=2$ and A'_0 has only two nonzero eigenvalues. Let $\boldsymbol{u}'_j$ be eigenvectors of A'_0, i.e.,

$$A'_0\boldsymbol{u}'_j=p_j\boldsymbol{u}'_j. \tag{3.54}$$

Then, we can arrange them such that $p_1\ge p_2>0$ and $p_j=0$ for $3\le j\le N_A-N_B$. Define

$$\boldsymbol{a}''_j=(\boldsymbol{a}'_1\cdots\boldsymbol{a}'_{N_A-N_B})\boldsymbol{u}'_j. \tag{3.55}$$

Then, we have $\boldsymbol{a}''_1\neq 0$, $\boldsymbol{a}''_2\neq 0$, and $\boldsymbol{a}''_j=0$ for $3\le j\le N_A-N_B$. We can define $\tilde{\boldsymbol{a}}_1$ and $\tilde{\boldsymbol{a}}_2$ as follows

$$\tilde{a}_1=\frac{1}{\sqrt{p_1}}\boldsymbol{a}''_1, \quad \tilde{a}_2=\frac{1}{\sqrt{p_2}}\boldsymbol{a}''_2. \tag{3.56}$$

Then we have $\tilde{a}_{1K'}=\tilde{a}^*_{1K}$, $\tilde{a}_{2K'}=\tilde{a}^*_{2K}$, and $|\tilde{\boldsymbol{a}}_1|=|\tilde{\boldsymbol{a}}_2|=1$.

By making another orthogonal transformation

$$t'_0=U't''U'^+, \tag{3.57}$$

with $U'=(\boldsymbol{u}'_1\,\boldsymbol{u}'_2\cdots\boldsymbol{u}'_{N_A-N_B})$, we have

$$t''_{ij}=\frac{1}{1-\zeta+\zeta p_j}\delta_{ij}. \tag{3.58}$$

Therefore, we have

$$t'_{ij}=\begin{cases}\displaystyle\sum_{k=1}^{N_A-N_B}\frac{u'_{ik}u'_{jk}}{1-\zeta+\zeta p_k} & (i,j\le N_A-N_B),\\ 0 & (i,j>N_A-N_B),\end{cases} \tag{3.59}$$

and

$$t^{AA}_{ij}=\sum_{l=1}^{N_A-N_B}\sum_{m=1}^{N_A-N_B}\sum_{k=1}^{N_A-N_B}\frac{u_{il}u'_{lk}u'_{mk}u_{mj}}{1-\zeta+\zeta p_k}. \tag{3.60}$$

Therefore, the T matrix is

$$\begin{aligned}
T^{AA}_S&=\sum_{i,j=1}^{N_A}\sum_{l=1}^{N_A-N_B}\sum_{m=1}^{N_A-N_B}\sum_{k=1}^{N_A-N_B}\frac{2\boldsymbol{a}_i u_{il}u'_{lk}u'_{mk}u_{mj}\boldsymbol{a}^+_j}{1-\zeta+\zeta p_k}\\
&=\frac{2p_1\tilde{\boldsymbol{a}}_1\tilde{\boldsymbol{a}}^+_1}{1-\zeta+\zeta p_1}+\frac{2p_2\tilde{\boldsymbol{a}}_2\tilde{\boldsymbol{a}}^+_2}{1-\zeta+\zeta p_2}.
\end{aligned} \tag{3.61}$$

This is formally the same expression as that of two

impurities at A sublattice points. Using eqs. (3.43) and (3.60), we have $t^{BA}=0$ and consequently $T^{BA}=0$. When the potential is sufficiently strong and $\zeta\approx 1$, the results become completely same as in the case of two strong impurities at A sublattice points.

When $N_A-N_B=2$, t'_0 becomes a $(2,2)$ matrix and therefore the T matrix becomes same as that of two impurities at A sublattice sites and is given by the above equation. When $N_A-N_B=1$, t'_0 is reduced to $(1,1)$ matrix and the T matrix becomes same as that of a single impurity at an A site. Therefore, we can conclude that in the limit $a/L\to 0$ the conductance vanishes, i.e., $G=0$, for $N_A-N_B\geq 2$, $G=e^2/\pi\hbar$ for $N_A-N_B=1$, and $G=2e^2/\pi\hbar$ for $N_A-N_B=0$. This explains results of recent elaborate numerical study.[39)]

§4. Numerical Results

As a first example, we consider a pair of nearest-neighbor A and B impurities, AB, located along the circumference direction in armchair nanotubes shown in Fig. 3(b). In this case, t_{KK}, $t_{K'K'}$, $r_{K'K}$, and $r_{KK'}$ are nonzero and other elements vanish identically as mentioned already. Figures 4 and 5 show numerical results of reflection and transmission coefficients as a function of $\tilde{u}$ for $n_c=20$ and 50, respectively, at $\varepsilon=0$. The lattice constant is chosen as $a=L/n_c$. For small $\tilde{u}$ both $|r_{K'K}|$ and $|r_{KK'}|$ increase with $\tilde{u}$ in proportion to $\tilde{u}$ in agreement with the lowest Born result given by a dotted line. At $\tilde{u}=|\tilde{u}_c|=\pi a/2\sqrt{3}L$ both $t_{K'K'}$ and $r_{K'K}$ exhibit a resonance behavior discussed in §3. For a sufficiently large value of $\tilde{u}$, both $|r_{K'K}|$ and $|r_{KK'}|$ approach a small value proportional to $(a/L)^2$. These results are in agreement with those of the analytical treatment discussed in the previous section.

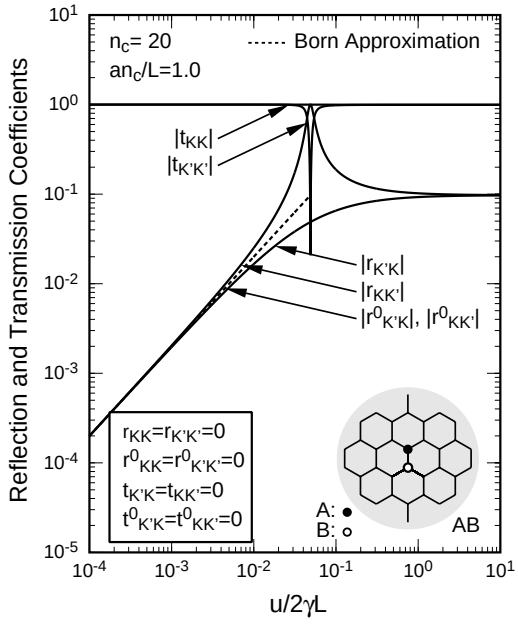

Fig. 4 Calculated reflection and transmission coefficients as a function of the potential strength $\tilde{u}=u/2\gamma L$ in the presence of a pair of nearest-neighbor AB impurities located along a circumference direction in armchair nanotubes. $n_c=20$ and $a/L=n_c^{-1}$.

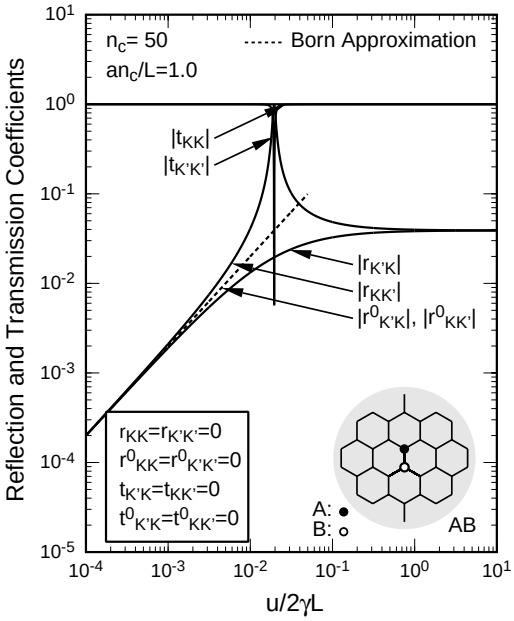

Fig. 5 Calculated reflection and transmission coefficients as a function of the potential strength $\tilde{u}=u/2\gamma L$ in the presence of a pair of nearest-neighbor AB impurities located along a circumference direction in armchair nanotubes. $n_c=50$ and $a/L=n_c^{-1}$.

Figure 6 shows results for three A impurities surrounding a single impurity located at a B site, A_3B, illustrated in Fig. 3(c) for $\varepsilon=0$. A resonance appears at a certain critical value of $\tilde{u}$, which is much more complicated than that of the AB pair. For $\tilde{u}$ smaller than the critical value all the reflection coefficients are essentially same as those of the lowest Born approximation. Above the critical value, $|r_{K'K}|$ $(=|r_{KK'}|)$ rapidly decreases with the increase of $\tilde{u}$, while $|r_{KK}|$ $(=|r_{K'K'}|)$ increases and approaches unity. Actually, $|r_{KK}|$ is almost the same as the dashed line corresponding to $|r_{KK}|$ for three impurities located at A sites surrounding the single B site, i.e. A_3 shown in Fig. 3(d).

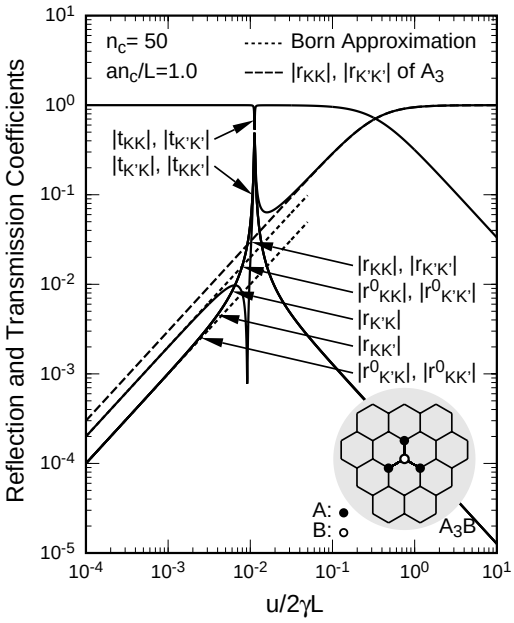

Fig. 7 Calculated reflection and transmission coefficients as a function of the potential strength $\tilde{u}=$

$u/2\gamma L$ in the presence of A_3B impurities in armchair nanotubes. $n_c = 50$ and $a/L = n_c^{-1}$. The dashed lines represent the results for A_3 impurities illustrated in Fig. 3(d).

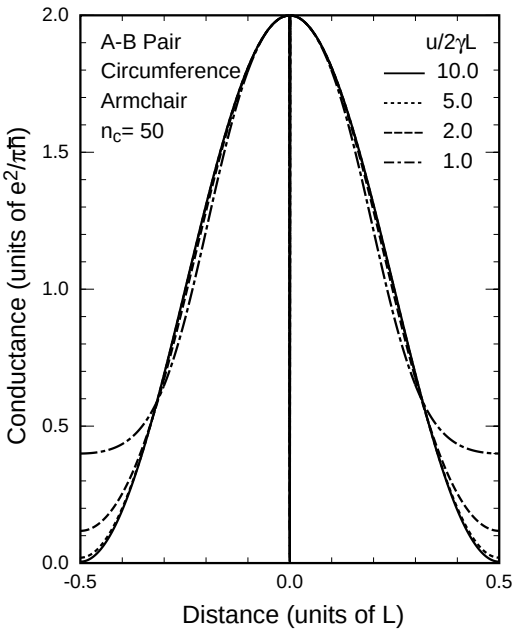

Fig. 8 Calculated conductance in the presence of a pair of A and B impurities along the circumference direction in an armchair nanotubes as a function of their distance d_{AB}. $n_c = 50$.

The origin of this behavior can easily be understood by looking at the structure of the lattice. In fact, when the local site energy at three A sites is sufficiently large, the B site surrounded by the three A sites is separated from the system and therefore the result should be independent of the energy at the B site. It is quite interesting that this is reproduced well even in the effective-mass scheme which takes into account the lattice structure only in the form of the matrix Schrödinger equation.

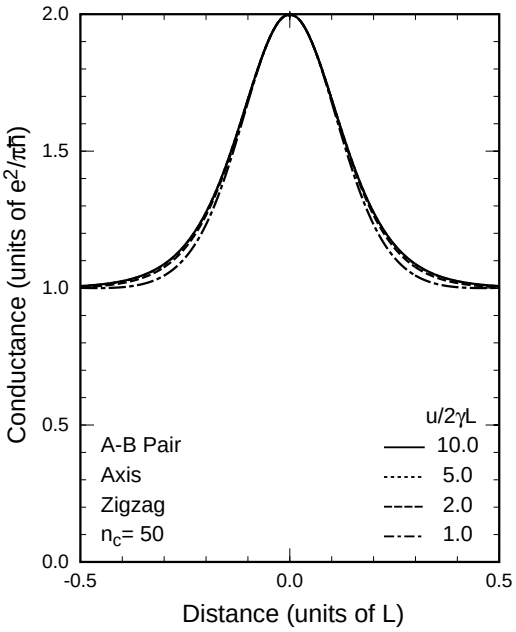

Fig. 9 Calculated conductance in the presence of a pair of A and B impurities along the axis direction in a zigzag nanotube as a function of their distance d_{AB}. $n_c = 50$.

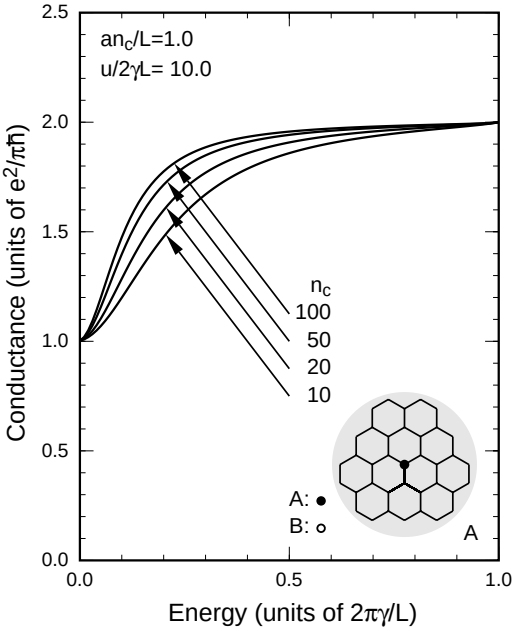

Fig. 10 Calculated conductance as a function of the Fermi energy in the presence of a strong impurity at an A site in an armchair nanotube illustrated in Fig. 3(a).

Figure 8 shows the conductance in the presence of a pair of A and B impurities along the circumference direction in an armchair nanotube as a function of their distance d_{AB}. The conductance is given by the ideal value $G = 2e^2/\pi\hbar$ for small d_{AB}, decreases with the increase of d_{AB}, and takes a minimum at $d_{AB} = L/2$. In the limit of a strong scatterer or a vacancy the minimum value vanishes, which is closely related to the fact that the vanishing of the off-diagonal Green's function $g_1(x, y)$ at $x = \pm L/2$ and $y = 0$.

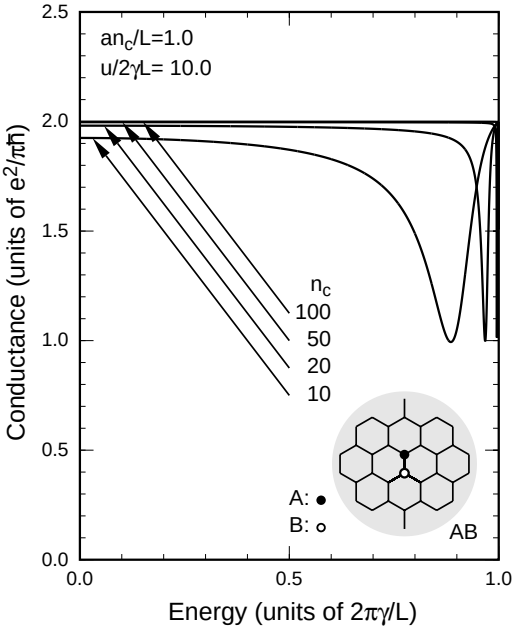

Fig. 11 Calculated conductance for an AB vacancy located in the circumference direction illustrated in

Fig. 3(b).

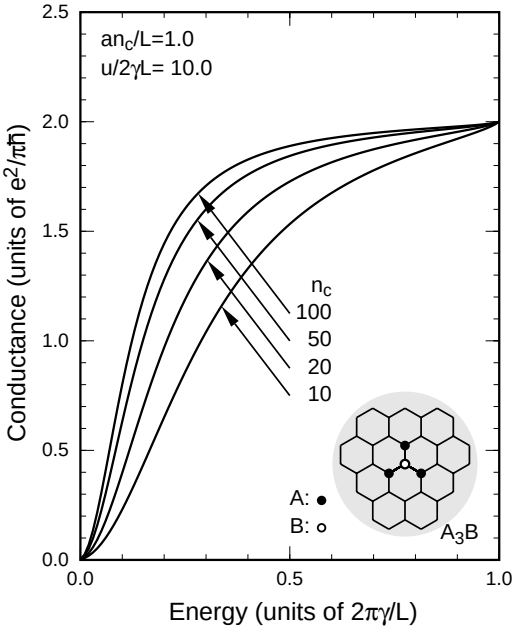

Fig. 12 Calculated conductance for an A_3B vacancy illustrated in Fig. 3(c).

At $d_{AB}=0$ the off-diagonal Green's function vanishes and eq. (3.27) gives immediately $t^{AA}=t^{BB}=1$ and $t^{AB}=t^{BA}=0$, which leads to the complete reflection or the vanishing conductance. When d_{AB} is comparable to or larger than the cutoff distance $a\sim L/n_c$, on the other hand, the off-diagonal Green's function becomes extremely large and the scattering is suppressed considerably, leading to the ideal conductance $G=2e^2/\pi\hbar$. Therefore, the conductance exhibits a singular behavior in the vicinity of $d_{AB}=0$. Actual lattices do not exhibit such a singular behavior because d_{AB} cannot be smaller than the cutoff distance $\sim L/n_c$.

Figure 9 shows the conductance in the presence of a pair of A and B impurities along the axis direction in a metallic zigzag nanotube as a function of their distance d_{AB}. The conductance is given by a value close to $G=2e^2/\pi\hbar$ for small d_{AB}, decreases with the increase of d_{AB}, and approaches a quantized value $G=e^2/\pi\hbar$ for a sufficiently large d_{AB}, i.e., $d_{AB}/L\sim 1$. This can be understood by the fact that $g_1(0,y)\approx -\mathrm{i}\,\mathrm{sgn}(y)$ for $|y|\gg L/\pi$.

Figure 10 shows the conductance as a function of the Fermi energy in the presence of a strong impurity at an A site in an armchair nanotube illustrated in Fig. 3(a). The conductance becomes the half of the ideal value $G=e^2/\pi\hbar$ at $\varepsilon=0$, increases gradually with the increase of ε, and reaches the ideal value $G=2e^2/\pi\hbar$ at $\varepsilon(2\pi\gamma/L)^{-1}=1$. The results are in agreement with those obtained in a tight-binding model[37] including the dependence on $n_c\sim L/a$.

Figure 11 shows the corresponding result for a pair of strong impurities located in the circumference direction illustrated in Fig. 3(b). The conductance is slightly smaller than the ideal value $G=2e^2/\pi\hbar$ and approaches it with the increase of $n_c\sim L/a$ except in the vicinity of $\varepsilon=2\pi\gamma/L$. Near $\varepsilon=2\pi\gamma/L$ the conductance exhibits a dip with $G=e^2/\pi\hbar$, which moves to the higher energy side with the increase of $n_c\sim L/a$. At $\varepsilon=2\pi\gamma/L$ the conductance recovers the ideal value $G=2e^2/\pi\hbar$. Figure 12 shows the result for the A_3B vacancy illustrated in Fig. 3(c). The conductance vanishes at $\varepsilon=0$ and reaches the ideal value $G=2e^2/\pi\hbar$ at $\varepsilon(2\pi\gamma/L)^{-1}=1$. These behaviors are again in agreement with those in a tight-binding model.[37]

§5. Discussion

We have shown analytically that in the limit of $a/L\to 0$ and a strong scatterer the conductance at $\varepsilon=0$ vanishes, i.e., $G=0$, for $|N_A-N_B|\geq 2$, $G=e^2/\pi\hbar$ for $|N_A-N_B|=1$, and $G=2e^2/\pi\hbar$ for $N_A-N_B=0$, where N_A and N_B are the number of impurities at A and B lattice sites, respectively. This may intuitively be understood in terms of a reduction of the scattering potential by multiple scattering from a pair of A and B scatterers. In fact, multiple scattering between an A impurity at $\boldsymbol{r}_i$ and a B impurity at $\boldsymbol{r}_j$ reduces their effective potential by the factor $\sim(\zeta g_0^{-1}\tilde{g}_{ij}^{AB}\boldsymbol{a}_i^+\boldsymbol{b}_j)^{-2}$. By eliminating AB pairs successively, some A or B impurities remain. The conductance is determined essentially by the number of these unpaired impurities.

Unfortunately, such a direct procedure is not rigorous mathematically. The reason is that there are many different ways in the elimination of AB pairs. Further, multiple scattering between unpaired and eliminated impurities cannot be neglected completely because of large off-diagonal Green's functions. The correct mathematical procedure given in §3.3 shows that a proper combination of A and B impurities lead to vanishing scattering potential and the residual potential is determined by another combination of remaining A or B impurities. This does not modify the fact that the conductance is determined by the number of remaining impurities, however.

Consider a pair of impurities at an A site $\boldsymbol{r}_A=(x_A,y_A)$ and a B site $\boldsymbol{r}_B=(x_B,y_B)$ closely spaced with each other and having a delta potential with strength u. For $\varepsilon=0$, the Schrödinger equation is given by

$$\begin{pmatrix} u_A(\boldsymbol{r}) & \mathrm{e}^{\mathrm{i}\phi_A}u_A(\boldsymbol{r}) & \gamma(\hat{k}_x-\mathrm{i}\hat{k}_y) & 0 \\ \mathrm{e}^{-\mathrm{i}\phi_A}u_A(\boldsymbol{r}) & u_A(\boldsymbol{r}) & 0 & \gamma(\hat{k}_x+\mathrm{i}\hat{k}_y) \\ \gamma(\hat{k}_x+\mathrm{i}\hat{k}_y) & 0 & u_B(\boldsymbol{r}) & \mathrm{e}^{\mathrm{i}\phi_B}u_B(\boldsymbol{r}) \\ 0 & \gamma(\hat{k}_x-\mathrm{i}\hat{k}_y) & \mathrm{e}^{-\mathrm{i}\phi_B}u_B(\boldsymbol{r}) & u_B(\boldsymbol{r}) \end{pmatrix}\begin{pmatrix} F^{KA} \\ F^{K'A} \\ F^{KB} \\ F^{K'B} \end{pmatrix}=0, \tag{5.1}$$

with $u_A(\boldsymbol{r})=u\delta(\boldsymbol{r}-\boldsymbol{r}_A)$ and $u_B(\boldsymbol{r})=u\delta(\boldsymbol{r}-\boldsymbol{r}_B)$. First, we should note that

$$\Big(\frac{\partial}{\mathrm{i}\partial x}+\mathrm{i}\frac{\partial}{\mathrm{i}\partial y}\Big)\frac{1}{z}=\Big(\frac{\partial}{\mathrm{i}\partial x}-\mathrm{i}\frac{\partial}{\mathrm{i}\partial y}\Big)\frac{1}{z^*}=-2\pi\mathrm{i}\delta(\boldsymbol{r}), \tag{5.2}$$

where $z=x+\mathrm{i}y$ and $z^*=x-\mathrm{i}y$. For a wave corresponding to the K point incident from the left hand side the above equation can be solved approximately by putting

$$\begin{aligned} F^{KA}&=\frac{1}{\sqrt{2AL}}\Big(1+f_A\frac{z_{AB}}{z-z_B}\Big), \\ F^{KB}&=\frac{\mathrm{i}}{\sqrt{2AL}}\Big(1+f_B\frac{z_{AB}^*}{z^*-z_A^*}\Big), \\ F^{K'A}&=\frac{1}{\sqrt{2AL}}f_A'\frac{z_{AB}^*}{z^*-z_B^*}, \\ F^{K'B}&=\frac{\mathrm{i}}{\sqrt{2AL}}f_B'\frac{z_{AB}}{z-z_A}, \end{aligned} \tag{5.3}$$

where $z_A=x_A+\mathrm{i}y_A$, $z_B=x_B+\mathrm{i}y_B$, and $z_{AB}=z_A-z_B$.

As long as f_A, f'_A, f_B, and f'_B are of the order of unity and $|z_{AB}|\sim a$, the correction terms proportional to $(z-z_A)^{-1}$, etc. are small except in the close vicinity of $\boldsymbol{r}_A$ or $\boldsymbol{r}_B$ and the above wave functions satisfy the periodic boundary conditions approximately in nanotubes with a large circumference $L/a\gg 1$. We have

$$\begin{pmatrix} u & u\mathrm{e}^{\mathrm{i}\phi_A} & 2\pi\gamma z^*_{AB} & 0 \\ u & u\mathrm{e}^{\mathrm{i}\phi_A} & 0 & 2\pi\gamma z_{AB}\mathrm{e}^{\mathrm{i}\phi_A} \\ 2\pi\gamma z_{AB} & 0 & u & u\mathrm{e}^{\mathrm{i}\phi_B} \\ 0 & 2\pi\gamma z^*_{AB}\mathrm{e}^{\mathrm{i}\phi_B} & u & u\mathrm{e}^{\mathrm{i}\phi_B} \end{pmatrix} \begin{pmatrix} f_A \\ f'_A \\ f_B \\ f'_B \end{pmatrix} = u \begin{pmatrix} -1 \\ -1 \\ 1 \\ 1 \end{pmatrix}. \tag{5.4}$$

This gives in the case $\tilde{u}=u/2\gamma L\gg 1$, in particular,

$$\begin{aligned} f_A &= \mathrm{e}^{\mathrm{i}\phi_B}\frac{z^*_{AB}}{z_{AB}}f'_A = -\frac{z^*_{AB}\mathrm{e}^{\mathrm{i}\phi_B}}{z_{AB}\mathrm{e}^{\mathrm{i}\phi_A}+z^*_{AB}\mathrm{e}^{\mathrm{i}\phi_B}}, \\ f_B &= \mathrm{e}^{\mathrm{i}\phi_A}\frac{z_{AB}}{z^*_{AB}}f'_B = +\frac{z_{AB}\mathrm{e}^{\mathrm{i}\phi_A}}{z_{AB}\mathrm{e}^{\mathrm{i}\phi_A}+z^*_{AB}\mathrm{e}^{\mathrm{i}\phi_B}}, \end{aligned} \tag{5.5}$$

which are independent of $\tilde{u}$ and are of the order of unity. It shows that the wave is transmitted without any reflection and effects of two strong impurities give only a small correction to the wave function except in the extreme vicinity of their positions.

For a given energy ε satisfying the condition (2.44), there are evanescent modes associated with bands with $n\neq 0$. Define the corresponding decay or growth rate $\pm k_n$ by

$$k_n = \sqrt{\kappa(n)^2-(\varepsilon/\gamma)^2}. \tag{5.6}$$

Then, evanescent modes are given by

$$\begin{aligned} \boldsymbol{F}^K_{n+}(\boldsymbol{r}) &= \frac{1}{\sqrt{LA}}\begin{pmatrix}\sqrt{1+k_n/\kappa(n)}\\ \sqrt{1-k_n/\kappa(n)}\end{pmatrix}\exp[-k_n y+\mathrm{i}\kappa(n)x], \\ \boldsymbol{F}^K_{n-}(\boldsymbol{r}) &= \frac{1}{\sqrt{LA}}\begin{pmatrix}\sqrt{1-k_n/\kappa(n)}\\ \sqrt{1+k_n/\kappa(n)}\end{pmatrix}\exp[+k_n y+\mathrm{i}\kappa(n)x], \end{aligned} \tag{5.7}$$

where $+$ denotes modes decaying in the positive y direction and $-$ in the negative y direction. This shows that when the energy approaches the bottom $2\pi\gamma/L$ of the first excited bands with $n=\pm 1$, the decay rate $k_{\pm 1}$ vanishes and the amplitude for A and B components becomes equal to each other. Therefore, the continuity of the wave function at $y=y_0$ is satisfied by including a single traveling mode

$$\boldsymbol{F}^K_{0+}(\boldsymbol{r}) = \frac{1}{\sqrt{LA}}\begin{pmatrix}1\\ \mathrm{i}\end{pmatrix}\exp(\mathrm{i}ky), \tag{5.8}$$

with $k=\varepsilon/\gamma$, and the evanescent modes $\boldsymbol{F}^K_{1+}$ and $\boldsymbol{F}^K_{1-}$ or $\boldsymbol{F}^K_{-1+}$ and $\boldsymbol{F}^K_{-1-}$, only. Further, by choosing the phase of the evanescent modes appropriately, the A or B component of the total wave function can be made vanish at an arbitrary value x_0 of the x coordinate. It means that such a wave is not affected by a short-range impurity located at (x_0,y_0) and is transmitted with probability one. The same is applicable to the wave function associated with the K' point. This is presumably the reason that the transmission coefficient always becomes unity at $\varepsilon=2\pi\gamma/L$ in the examples of the numerical results shown in §4.

Consider the case that n impurities V_j $(j=1,\ldots,n)$ are located at A sites within the distance much smaller than L. In this case, only the diagonal Green's function g_0 appears in the perturbation series for the T matrix. Because g_0 does not vary with the distance so much, it can be replaced by that for $x=y=0$. Then, the T matrix is calculated as

$$\begin{aligned} (\alpha|T|\beta) =& \boldsymbol{f}^+_\alpha\Big[1-\sum_{j'}\frac{1}{AL}V_{j'}G\Big]^{-1}\sum_j\frac{1}{AL}V_j\boldsymbol{f}_\beta \\ &\times\exp[-\mathrm{i}(\kappa_\alpha-\kappa_\beta)x_0-\mathrm{i}(k_\alpha-k_\beta)y_0], \end{aligned} \tag{5.9}$$

where (x_0,y_0) is the center-of-mass of impurities. This result shows that the effective potential is given by the sum of the potential of each impurity. The same is true of the case of impurities at B sites. It is possible therefore to derive the results obtained in §3 for vacancies consisting of same sublattice points using eq. (5.9).

It would be expected, intuitively, that for a pair of nearest-neighbor A and B impurities, their positions may be regarded as same because the distance is much smaller than the typical electron wavelength which is actually infinite at $\varepsilon=0$. Because of the singularity of the off-diagonal Green's function, such an approximate procedure becomes completely invalid when impurities at A and B sites coexist, except in the case that the potential is weak and the lowest Born approximation is appropriate.

Acknowledgments

This work was supported in part by Grants-in-Aid for Scientific Research and Priority Area, Fullerene Network, from Ministry of Education, Science and Culture. One of the authors (T.N.) acknowledges the support of a fellowship from Special Postdoctoral Researches Program at RIKEN. One of the authors (M.I.) has been supported by Research Fellowships of the Japan Society for the Promotion of Science for Young Scientists. Numerical calculations were performed in part on FACOM VPP500 in Supercomputer Center, Institute for Solid State Physics, University of Tokyo and in Institute of Physical and Chemical Research.

1) S. Iijima: Nature (London) **354** (1991) 56.
2) S. Iijima and T. Ichihashi: Nature (London) **363** (1993) 603.
3) D. S. Bethune, C. H. Kiang, M. S. de Vries, G. Gorman, R. Savoy, J. Vazquez and R. Beyers: Nature (London) **363** (1993) 605.
4) N. Hamada, S. Sawada and A. Oshiyama: Phys. Rev. Lett. **68** (1992) 1579.
5) J.W. Mintmire, B.I. Dunlap and C.T. White: Phys. Rev. Lett. **68** (1992) 631.
6) R. Saito, M. Fujita, G. Dresselhaus and M. S. Dresselhaus: Phys. Rev. B **46** (1992) 1804; Appl. Phys. Lett. **60** (1992) 2204.
7) M. S. Dresselhaus, G. Dresselhaus and R. Saito: Phys. Rev. B **45** (1992) 6234.
8) R. A. Jishi, M. S. Dresselhaus and G. Dresselhaus: Phys. Rev. B **47** (1993) 16671.
9) K. Tanaka, K. Okahara, M. Okada and T. Yamabe: Chem. Phys. Lett. **191** (1992) 469.
10) Y. D. Gao and W. C. Herndon: Mol. Phys. **77** (1992) 585.
11) D. H. Robertson, D. W. Berenner and J. W. Mintmire: Phys. Rev. B **45** (1992) 12592.
12) C. T. White, D. C. Robertson and J. W. Mintmire:

Phys. Rev. B **47** (1993) 5485.
13) H. Ajiki and T. Ando: J. Phys. Soc. Jpn. **62** (1993) 1255; *ibid* **65** (1996) 505.
14) H. Ajiki and T. Ando: J. Phys. Soc. Jpn. **62** (1993) 2470; *ibid* **64** (1995) 4382.
15) H. Ajiki and T. Ando: Physica B **201** (1994) 349; Jpn. J. Appl. Phys. Suppl. **34** (1995) 107.
16) T. Ando: J. Phys. Soc. Jpn. **66** (1997) 1066.
17) N. A. Viet, H. Ajiki and T. Ando: J. Phys. Soc. Jpn. **63** (1994) 3036.
18) H. Ajiki and T. Ando: J. Phys. Soc. Jpn. **64** (1995) 260.
19) S. N. Song, X. K. Wang, R. P. H. Chang and J. B. Ketterson: Phys. Rev. Lett. **72** (1994) 697.
20) L. Langer, V. Bayot, E. Grive, J. -P. Issi, J. P. Heremans, C. H. Olk, L. Stockman, C. Van Haesendonck and Y. Brunseraede: Phys. Rev. Lett. **76** (1996) 479.
21) F. Katayama, Master thesis (Univ. Tokyo, 1996).
22) W. -D. Tian and S. Datta: Phys. Rev. B **49** (1994) 5097.
23) R. Saito, G. Dresselhaus and M. S. Dresselhaus: Phys. Rev. B **53** (1996) 2044.
24) R. Tamura and M. Tsukada: Solid State Commun. **101** (1997) 601; Phys. Rev. B **55** (1997) 4991.
25) T. Nakanishi and T. Ando: J. Phys. Soc. Jpn. **66** (1997) 2973.
26) H. Matsumura and T. Ando: J. Phys. Soc. Jpn. **67** (1998) 3542.
27) Y. Miyamoto, S. G. Louie and M. L. Cohen, Phys. Rev. Lett. **76** (1996) 2121.
28) L. Chico, L. X. Benedict, S. G. Louie and M. L. Cohen: Phys. Rev. B **54** (1996) 2600.
29) T. Seri and T. Ando: J. Phys. Soc. Jpn. **66** (1997) 169.
30) T. Ando and T. Seri: J. Phys. Soc. Jpn. **66** (1997) 3558.
31) N. H. Shon and T. Ando: J. Phys. Soc. Jpn. **67** (1998) 2421.
32) T. Ando and T. Nakanishi: J. Phys. Soc. Jpn. **67** (1998) 1704.
33) T. Ando, T. Nakanishi and R. Saito: J. Phys. Soc. Jpn. **67** (1998) 2857.
34) T. Nakanishi and T. Ando: J. Phys. Soc. Jpn. **68** (1999) 561.
35) T. Ando, T. Nakanishi and R. Saito: Microelectronic Engineering **47** (1999) 421.
36) S. Frank, P. Poncharal, Z. L. Wang and W. A. de Heer: Science **280** (1998) 1744.
37) M. Igami, T. Nakanishi and T. Ando: J. Phys. Soc. Jpn. **68** (1999) 716.
38) M. Igami, T. Nakanishi and T. Ando: Mol. Cryst. Liq. Cryst. (in press).
39) M. Igami, T. Nakanishi and T. Ando: J. Phys. Soc. Jpn. **68** (1999) No. 10.
40) T. Nakanishi, M. Igami and T. Ando: Physica E (in press).